Energy-Efficient Multi-Access Edge Computing for Heterogeneous Satellite-Maritime Networks: A Hybrid Harvesting-and-Offloading Design

Minghui Dai ⓘ, *Member, IEEE*, Shan Chang ⓘ, *Member, IEEE*, Yixuan Wang, and Zhou Su ⓘ, *Senior Member, IEEE*

Abstract—Low earth orbit (LEO) constellation integrated maritime networks have recently attracted much interest due to the rapid development of maritime applications and services. LEO satellites have the advantages of wide coverage to provide seamless connection for maritime wireless devices. However, due to the limited battery and computing capacity of uncrewed aerial vehicles (UAVs) for ocean information perception and processing, the computing-intensive and delay-sensitive oceanic data suffer from long latency and high energy consumption, which degrades the efficiency of maritime services. In this paper, to enhance the perception and offloading endurance of UAVs in maritime networks, we propose an energy efficient multi-access edge computing scheme for heterogeneous satellite-maritime networks, with the objective of minimizing the cumulative transmitted energy for UAVs. Specifically, we first present a heterogeneous satellite-maritime network framework in which LEO satellites and uncrewed surface vehicles (USVs) equipped with edge servers can process workloads simultaneously. Next, considering the limited battery supply of UAVs, we propose a hybrid harvesting-and-offloading scheme for resource allocation, where UAVs first harvest energy from solar power and radio frequency power from USV, and then UAVs determine the offloading strategy for task processing. Moreover, a joint optimization problem is formulated to optimize the offloading decision, the time scheduling, and the transmitting power. We also exploit a vertical architecture to solve the formulated problem. Regarding each decomposed sub-problem, we propose efficient algorithms to derive the corresponding solutions. Finally, we provide numerical results to validate the performance of our proposed algorithms in comparison with several benchmark algorithms.

Index Terms—Heterogeneous satellite-maritime networks, multi-access edge computing, and energy efficient design.

I. INTRODUCTION

W ITH the increasing demands of maritime resource exploration, high-throughput and low-latency maritime communication networks have attracted growing interest from academia and industry in recent years [1], [2]. Thanks to the advancement of satellite technology, the integration of satellite and maritime networks is a promising paradigm to achieve seamless access and provide increased network resources for maritime wireless devices [3], [4]. Additionally, the significant advantages (e.g., small propagation loss and low propagation delay) of low earth orbit (LEO) satellites produce the paradigm of LEO constellation networks. The LEO satellite communication networks can achieve large coverage for ocean areas. The satellite links are less susceptible to marine environmental factors, which can guarantee stable communication quality and can provide reliable communication support for maritime emergency scenario such as maritime searching and rescuing. Thus, the LEO constellation networks pave the way to extend the terrestrial and maritime services to the space, which enables a wide range of maritime applications (e.g., ocean remote sensing, sea navigation) and creates a new paradigm for services (e.g., space backhaul and reconnaissance) [5]. However, due to the large amount of ocean data, the requirements for high computing and communication resources in satellite-maritime networks are critical issues to achieve high quality maritime services.

Multi-access edge computing is an efficient resource allocation scheme, which can greatly improve the resource utilization in maritime networks. Thanks to the flexibility and ease of deployment of uncrewed aerial vehicles (UAVs), it can perceive a wide range of ocean information in the air [6], [7], [8]. The collected data by UAVs can be processed locally and can be offloaded to maritime edge devices via multi-access. Satellite in-orbit computing is considered as a computing carrier for the future maritime networks. By embedding edge servers in satellites, oceanic data can be uploaded to satellites for processing. Moreover, in response to complex maritime mission requirements such as searching and rescuing or patrol operations, uncrewed surface vehicles (USVs) can be rapidly deployed to support task execution. USVs equipped with computing capacities can also process data locally in the sea. However, there are also several challenges for data processing in satellite-maritime networks. On one hand, when numerous maritime devices (e.g., UAVs, ships) simultaneously transmit data workloads to a satellite, it may lead to overload of the space link. This overload subsequently results in network congestion and prolonged transmission delay. On the other hand, due to the limitation of on-board battery capacity of UAVs, it is difficult for UAVs to support long duration data offloading in the air. Therefore, the energy

consumption should be investigated to improve the efficiency of maritime edge computing.

Wireless power transfer (WPT) has been envisioned as an effective energy harvesting technology for mobile terminal devices [9], [10]. In maritime networks, since UAVs cannot meet the requirements for long-term ocean exploration, it impacts the sustained stability of maritime operations and the effectiveness of emergency response. Moreover, during ocean resource exploration, it is difficult to replace or recharge UAVs quickly in complex ocean environment. USVs can serve as mobile charging platforms to replenish UAVs' energy in the ocean. Thanks to WPT technology, UAVs can extract energy from the received radio frequency signals for energy harvesting, which thus extends the endurance of UAVs [11], [12]. In addition, UAVs generally have restricted computation resources, which cannot process a large number of perception tasks. Thus, the emerging wireless-powered edge computing technology by integrating WPT with multi-access for USVs and satellites holds the potential to address the limitations of constrained computing resource and energy shortages. This enhances the sustainability of the system and effectively extends the UAV's flight duration and operational period and reduces data processing delay [13]. There have been many works focusing on optimizing WPT performance in maritime networks [14], [15]. The trajectory optimization in UAV-assisted WPT networks is proposed in [16] to minimize the energy consumption. The design of UAV-aided WPT and data collection is presented in [6] with the objective of reducing the outage probability. The UAV-empowered WPT network is studied in [17] to charge all devices on the ground periodically while minimizing the average UAV energy consumption. The above mentioned studies have investigated the UAV-assisted WPT system for prolonging the sustainable time of wireless devices. However, the energy harvesting and offloading schemes in maritime environment are still crucial issues that should be well investigated.

Motivated by the above considerations, we propose an energy efficient multi-access computing offloading scheme for heterogeneous satellite-maritime networks, with the objective of improving the computing efficiency and minimizing the energy consumption. The main contributions of this work are as follows.

- *Integrated Satellite-Maritime Edge Computing Framework:* By leveraging the resources of in-orbit computing and surface edge computing, we present a heterogeneous satellite-maritime edge computing framework in which both satellites and USVs equipped with edge servers can process the offloading tasks. To save the energy consumption of UAVs, we consider that the data collected by UAVs can be simultaneously offloaded to LEO satellite and USV for processing via UAV-to-satellite link and UAV-to-USV link, respectively. The orthogonal frequency division multiplexing (OFDM) technology is adopted to avoid the co-channel interference.

- *Energy Efficient Multi-Access Task Offloading Scheme:* In order to improve the offloading endurance and efficiency, we design a hybrid harvesting-and-offloading multi-access task offloading scheme, which consists of the WPT duration and the computation offloading duration. We formulate

a joint optimization problem to minimize the cumulative transmitted energy of all UAVs by optimizing the offloading decision, the time scheduling, and the transmitting power. A vertical decomposition approach is exploited to solve the formulated problem. We propose corresponding algorithms to derive the optimal solutions.

- *Performance Evaluation:* We finally provide extensive numerical results to evaluate the performance of our proposed algorithms. The results show that the proposed algorithms can obtain the optimal solutions for task offloading, and can significantly reduce the energy consumption in comparison with several benchmark algorithms.

The remainder of this paper is organized as follows. Section II reviews the related studies. Section III presents the system model and problem formulation. Section IV provides the proposed algorithms to solve the formulated problems. Numerical results are shown in Section V to validate the performance of the proposed algorithms. Section VI closes this paper with conclusions and future works.

II. LITERATURE REVIEW

This section reviews the literature studies focusing on the framework design of satellite-maritime integrated networks with its resource allocation scheme. Satellite-maritime integrated networks have been considered as the effective network framework to provide various maritime services, which also attract much attention from academia and industry. Zong et al. [18] presented a satellite-marine environmental monitoring system for transmission control. The proposed scheme improves the efficiency of maritime data collection. Dai et al. [27] investigated a multi-access computation offloading scheme in maritime networks to minimize the energy consumption of ocean devices. A collaborative transmission architecture is introduced by [24] in maritime networks for minimizing the system latency. Cai et al. [19] studied the access control problem in satellite-based marine Internet of Things networks, with the objective of minimizing the long-term peak age of information. Zeng et al. [28] designed the USV-assisted maritime-satellite wireless networks, and a joint optimization problem is formulated to obtain the optimal cooperative beamforming and trajectory while maximizing the system throughput. Garibotto et al. [20] conducted the performance analysis for cruise ships over the satellite networks. Li et al. [22] proposed the UAV-enabled maritime coverage enhancement in satellite-terrestrial maritime networks in which the UAV trajectory and transmission power are jointly optimized. Fang et al. [29] proposed a hybrid multi-access satellite-UAV-terrestrial network and formulated an optimization problem to maximize the sum rate of the network. Xu et al. [30] developed on-demand resource scheduling scheme in space-air-ocean integrated networks to achieve reliable services. Cheng et al. [25] investigated the relay placement of maritime devices for satisfying the requirement of frame error rate. Zeng et al. [26] introduced the marine communication system to maximize the throughput of USVs. Lin et al. [31] investigated path planning in software-defined networking-assisted maritime edge computing networks. Zeng et al. [23] introduced the UAV

TABLE I
COMPARISON OF EXISTING WORKS AND OUR PROPOSAL

Network Architecture	Versatility			Efficiency		CWPT[1]
	Multi-access	Cooperation	Postback result	Sustainability	Overhead	
Satellite-based networks [18], [19], [20], [21]	✓	×	×	Medium	Medium	×
UAV-based networks [6], [7], [22], [23]	✓	✓	×	Low	High	×
Maritime-based networks [24], [25], [26]	✓	✓	×	Low	Medium	×
Our proposal	✓	✓	✓	**High**	**Low**	✓

[1] "CWPT" means "Customized for Wireless Power Transfer" (customized to meet the requirements of charging).

and USV collaborative framework for task offloading to minimize the total computing delay. Hu et al. [21] proposed the LEO-enabled shore-to-ship communication networks to improve the transmission performance.

Ma et al. [32] proposed a novel one-to-many charging scheme that enables mobile charger to simultaneously charge multiple sensors. Sun et al. [33] considered the rechargeable wireless sensor networks with multiple mobile chargers to optimize the power allocation strategy. Mahmoodi et al. [34] utilized the solar-powered underwater vehicles to collect marine data, and a three-dimensional trajectory optimization problem is exploited with the objective of maximizing the harvested energy. Yuan et al. [35] investigated the UAV-enabled WPT networks from the prospect of energy-efficient design. Tun et al. [36] presented a collaborative multi-UAV-assisted edge computing framework to minimize the total latency of users by optimizing the computing and communication resources. The data offloading for UAV-aided multi-access edge computing scheme was proposed in [37] to determine the available computing choices. Diao et al. [38] proposed the UAV-relaying-assisted edge computing system to jointly optimize the offloading and scheduling strategies, with the objective of minimizing the energy consumption of UAV. Peng et al. [39] investigated the UAV-assisted edge computing to determine the resource allocation strategy while satisfying the quality of service requirement. Kim et al. [40] investigated the wireless power and the trajectory optimization for UAV-enabled networks. Singh et al. [15] introduced UAV-aided wireless networks to provide desired power to ground users. Pan et al. [41] proposed the UAV-empowered energy transfer scheme for ground devices for improving the energy utilization. Ning et al. [42] introduced the UAV-enabled energy harvesting scheme by jointly optimizing the resource allocation. Zhao et al. [43] studied the wireless powered UAV networks for maximizing the transmission data size via optimizing the energy transfer strategy.

The limited communication and computing resources restrict the application of maritime services. Existing works have discussed the resource allocation strategy in satellite-terrestrial integrated networks, and different schemes have been proposed to optimize the network performance from the perspective of energy consumption and latency. Different from above-mentioned works, this paper focuses on the design of hybrid harvesting-and-offloading scheme in multi-access satellite-maritime networks, with the objective of minimizing the energy consumption via optimizing the resource allocation. The comparison of existing works and our proposal is illustrated in Table I.
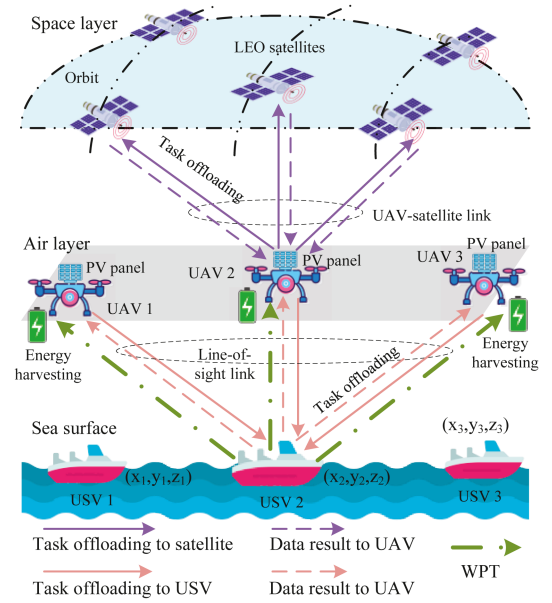

Fig. 1. The scenario of energy efficient multi-access computing offloading for heterogeneous satellite-maritime networks.

III. SYSTEM MODEL AND PROBLEM FORMULATION

This section first illustrates the system model. Then, the satellite-maritime communication model is presented, followed by the harvesting and offloading model. Finally, we present the formulated problem.

A. System Model

As shown in Fig. 1, we consider the heterogeneous wireless powered satellite-maritime networks, which consist of the surface layer, the aerial layer and the space layer. In aerial layer, a cluster of UAVs is designated to collect ocean data within a specific area. We use $\mathcal{I} = \{1, 2, \ldots, I\}$ to express the set of UAVs in a disjoint air area. The set of sensing tasks of UAVs is denoted as $\mathcal{M} = \{m_1, m_2, \ldots, m_I\}$. The total workload of UAV i is denoted by $S_{m_i}^{\text{tot}}$. Due to the limited communication and computing resources, UAVs can process their tasks locally or partially offload tasks to USVs or LEO satellites [44]. We consider a multi-access offloading strategy for UAVs, i.e., UAVs can offload different parts of workloads to respective edge nodes for processing [45]. We use $s_{m_i}^{\text{off}}$ to denote the offloading workload size of UAV i. In order to save the energy of UAVs, we consider a hybrid harvesting-and-offloading scheme, i.e., UAVs

TABLE II
KEY NOTATIONS USED IN THIS PAPER

Notation	Definition	Notation	Definition
$S_{m_i}^{\text{tot}}$	Total workloads of UAV i	$\hat{E}_{i,k}^{\text{Ph-II}}$	Energy consumption for UAV i to offload data to satellite k
$s_{m_i}^{\text{off}}$	Offloading workloads of UAV i	$t_j^{\text{Ph-III}}$	Local computing delay of USV j in Phase III
G_i	Antenna gain of UAV i	$\hat{t}_k^{\text{Ph-III}}$	Local computing delay of satellite k in Phase III
$\hat{G}_k$	Antenna gain of satellite k	$t_{j,i}^{\text{Ph-IV}}$	Data downloading delay from USV j to UAV i in Phase IV
τ_i^{H}	Energy harvesting time for UAV i	$\hat{t}_{k,i}^{\text{Ph-IV}}$	Data downloading delay from satellite k to UAV i in Phase IV
$t_i^{\text{Ph-I}}$	Local computing delay of UAV i in Phase I	E_i^{H}	Harvested energy for UAV i in WPT duration
$E_i^{\text{Ph-I}}$	Local energy consumption of UAV i in Phase I	E_i^{PV}	Harvested solar energy of UAV i
$t_{i,j}^{\text{Ph-II}}$	Data uploading delay from UAV i to USV j in Phase II	E_i^{hov}	Hovering energy consumption of UAV i
$E_{i,j}^{\text{Ph-II}}$	Energy consumption for UAV i to offload data to USV j	t_i^{ove}	Overall delay for completing the workload of UAV i
$\hat{t}_{i,k}^{\text{Ph-II}}$	Data uploading delay from UAV i to satellite k in Phase II	E_i^{ove}	Overall consumption for completing the workload of UAV i

first harvest energy from radio frequency power and solar energy, and then UAVs offload their tasks for processing. For the sake of clear presentation, the key notations used in this paper are summarized in Table II.

In surface layer, we use $\mathcal{J} = \{1, 2, \ldots, J\}$ to denote the set of USVs in a disjoint ocean area. Each USV is equipped with an edge computing server for task processing in the surface [46]. We use a binary variable $x_j(m_i) \in \{0, 1\}$ to indicate whether UAV i's workload is offloaded to USV j or not. Here, $x_j(m_i) = 1$ means that UAV i offloads workload $s_{m_i}^{\text{off}}$ to USV j, otherwise $x_j(m_i) = 0$. We consider that each USV is equipped with an energy transmitter for charging UAVs through broadcasting radio frequency power.

In space layer, we consider an ultra-dense LEO satellite network, in which multiple LEO satellites are covering the UAVs during a time slot [47]. We use $\mathcal{K} = \{1, 2, \ldots, K\}$ to denote the set of LEO satellites. The satellite equipped with edge servers can process the received data and transmit results to UAVs. Each UAV can choose a proper satellite to process its data. We use a binary variable $\hat{x}_k(m_i) \in \{0, 1\}$ to denote the offloading decision of satellite k. $\hat{x}_k(m_i) = 1$ means that UAV i offloads workload $s_{m_i}^{\text{off}}$ to satellite k, otherwise $\hat{x}_k(m_i) = 0$. Based on the above modeling, the offloading strategy of UAV i for each task m_i can be expressed as

$$S_{m_i}^{\text{tot}} = \underbrace{\left(S_{m_i}^{\text{tot}} - s_{m_i}^{\text{off}}\right)}_{\text{local computing size}} + \underbrace{s_{m_i}^{\text{off}}\left(x_j(m_i) + \hat{x}_k(m_i)\right)}_{\text{offloading computing decision}},$$
$$\forall i \in \mathcal{I}, \forall j \in \mathcal{J}, \forall k \in \mathcal{K}. \quad (1)$$

Since the offloading workload cannot be executed by USV and satellite at the same time, we have $x_j(m_i) = 1$ if and only if $\hat{x}_k(m_i) = 0$, and vice versa.

B. Satellite-Maritime Communication Model

UAVs can communicate with both USVs and LEO satellites for data offloading in maritime networks. We consider two channel models including the UAV-to-satellite link and the UAV-to-USV link.

As shown in Fig. 2, the available communication time between UAV and satellite can be obtained based on geometric
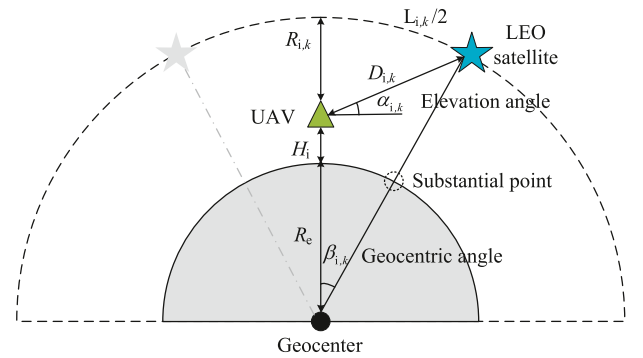

Fig. 2. The geometric relationship for LEO satellite and UAV.

relationship [48]. The elevation angle between UAV i and an LEO satellite k can be expressed as

$$\alpha_{i,k} = \arccos\left(\frac{R_e + H_i + R_{i,k}}{D_{i,k}} \sin \beta_{i,k}\right), \forall i \in \mathcal{I}, \forall k \in \mathcal{K}, \quad (2)$$

where parameter R_e denotes the radius of the earth. Parameter H_i means the hovering height of UAV i. Parameter $R_{i,k}$ is the distance between UAV i and satellite k's orbit. Parameter $D_{i,k}$ expresses the distance between UAV i and satellite k. $\beta_{i,k}$ indicates the geocentric angle corresponding to the satellite coverage area, which can be expressed as

$$\beta_{i,k} = \arccos\left(\frac{R_e + H_i}{R_e + H_i + R_{i,k}} \cos \alpha_{i,k}\right) - \alpha_{i,k},$$
$$\forall i \in \mathcal{I}, \forall k \in \mathcal{K}. \quad (3)$$

Let $L_{i,k}$ denote the arc length that UAV i can communicate with the LEO satellite k. We can obtain $L_{i,k} = 2(R_e + H_i + R_{i,k})\beta_{i,k}$. Let v_k denote the speed of LEO satellite k. We can express the available communication time between UAV and satellite as

$$t_{i,k}^{\text{UAV}} = \frac{L_{i,k}}{v_k}, \forall i \in \mathcal{I}, \forall k \in \mathcal{K}. \quad (4)$$

For data uplink transmission between UAV and satellite, based on [49], the channel between satellite and UAV is modeled by

the Weibull channel model (which is mainly affected by the rain attenuation). Let $\hat{G}_k$ and G_i denote the antenna gains of satellite k and UAV i, respectively. We can express the power attenuation of uplink from UAV i to satellite k as

$$\hat{g}_{i,k}^{\text{UAV}} = \frac{G_i \hat{G}_k \lambda^2}{(4\pi D_{i,k})^2} 10^{-\frac{\theta_{\text{rain}}}{10}}, \forall i \in \mathcal{I}, \forall k \in \mathcal{K}, \quad (5)$$

where parameter λ denotes the wavelength of carrier. θ_{rain} means the rain attenuation which follows the Weibull distribution.

To avoid the data uploading overlapping, we consider the OFDM technology, which divides the bandwidth for UAV-satellite uplinks into a group of orthogonal subchannels. According to the Shannon equation, we can express the achievable transmission rate from UAV i to satellite k as

$$\hat{r}_{i,k}^{\text{UAV}} = \hat{W}_k^{\text{up}} \log_2 \left(1 + \frac{\hat{p}_{i,k}^{\text{UAV}} \hat{g}_{i,k}^{\text{UAV}}}{\hat{W}_k^{\text{up}} \sigma_k^2} \right), \forall i \in \mathcal{I}, \forall k \in \mathcal{K}, \quad (6)$$

where parameter $\hat{W}_k^{\text{up}}$ means the allocated bandwidth by satellite k. Parameter $\hat{p}_{i,k}^{\text{UAV}}$ is the transmission power of UAV i to satellite k. Parameter σ_k^2 denotes the background noise power at satellite k.

For data transmission between UAV and USV, the channels from UAV to USV are mainly dominated by line-of-sight links. Considering the mobility of UAVs and USVs, we adopt the three-dimensional coordinate system. The coordinate of UAV i is $\mathbf{q}_i \in \mathbb{R}^3$, which can be denoted by $\mathbf{q}_i = \{x_i, y_i, H_i\}$. We can also denote the coordinate of USV j as $\hat{\mathbf{q}}_j \in \mathbb{R}^3$, which is expressed by $\hat{\mathbf{q}}_j = \{\hat{x}_j, \hat{y}_j, \hat{z}_j\}$. Taking the time-varying into account, for each UAV i, the movement trajectory is constrained by $\|\mathbf{q}_i(\iota+1) - \mathbf{q}_i(\iota)\|^2 \leq (\iota \vartheta_i^{\max})^2$. Here, ι denotes the time slot. $\vartheta_i^{\max}$ means the maximum speed of UAV i. Similarly, the movement trajectory for USV j can be expressed as $\|\hat{\mathbf{q}}_j(\iota+1) - \hat{\mathbf{q}}_j(\iota)\|^2 \leq (\iota \vartheta_j^{\max})^2$, where $\hat{\vartheta}_j^{\max}$ indicates the maximum speed of USV j.

The distance between UAV i and USV j can be obtained by $d_{i,j} = \|\mathbf{q}_i - \hat{\mathbf{q}}_j\|$. We can express the channel gain between UAV i and USV j as

$$\tilde{g}_{i,j}^{\text{UAV}} = \delta_0 d_{i,j}^{-2} = \frac{\delta_0}{\|\mathbf{q}_i - \hat{\mathbf{q}}_j\|^2}, \forall i \in \mathcal{I}, \forall j \in \mathcal{J}, \quad (7)$$

where parameter δ_0 denotes the channel power gain at the reference distance of $d_0 = 1$m. In order to avoid collision, we consider that UAVs cannot fly too close to USVs, and we use $d^{\min}$ to denote the minimum safe distance between UAVs and USVs for collision avoidance. The channel gain between UAV i and USV j can be modified as

$$g_{i,j}^{\text{UAV}} = \frac{\delta_0}{\max \left\{ (d^{\min})^2, \|\mathbf{q}_i - \hat{\mathbf{q}}_j\|^2 \right\}}, \forall i \in \mathcal{I}, \forall j \in \mathcal{J}. \quad (8)$$

Let $p_{i,j}^{\text{UAV}}$ denote the transmission power of UAV i to USV j. We can express the achievable transmission rate from UAV i to USV j as

$$r_{i,j}^{\text{UAV}} = W_j^{\text{up}} \log_2 \left(1 + \frac{p_{i,j}^{\text{UAV}} g_{i,j}^{\text{UAV}}}{W_j^{\text{up}} \sigma_j^2} \right), \forall i \in \mathcal{I}, \forall j \in \mathcal{J}, \quad (9)$$
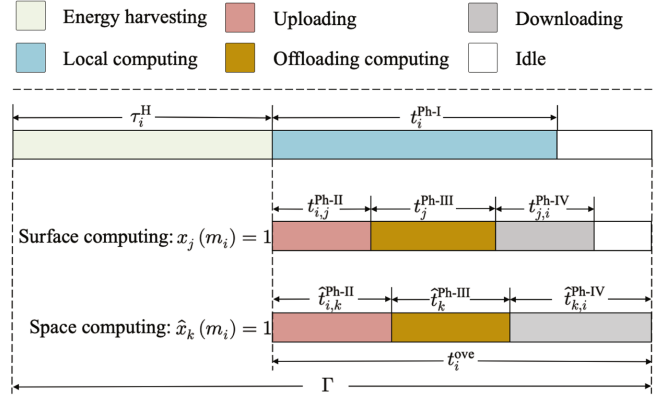

Fig. 3. Time scheduling of harvesting-and-offloading for multi-access computing.

where parameter W_j^{up} denotes the allocated bandwidth by USV j. σ_j^2 expresses the background noise power at USV j.

C. Harvesting and Offloading Model

As depicted in Fig. 3, we consider a complete cycle for performing UAVs' tasks as an episode (the length of episode is denoted by Γ). An episode of length Γ consists of two frames including the harvesting duration and the offloading duration. The former is the energy harvesting time for UAV, denoted by τ_i^{H}. The latter is divided into four time slots: The first time slot is the local computing time by UAV, denoted by $t_i^{\text{Ph-I}}$. The second time slot is the uploading time from UAV to USV and satellite, denoted by $t_{i,j}^{\text{Ph-II}}$ (in the case of $x_j(m_i) = 1$) and $\hat{t}_{i,k}^{\text{Ph-II}}$ (in the case of $\hat{x}_k(m_i) = 1$). The third time slot is the computing delay by USV and LEO satellite, denoted by $t_j^{\text{Ph-III}}$ (in the case of $x_j(m_i) = 1$) and $\hat{t}_k^{\text{Ph-III}}$ (in the case of $\hat{x}_k(m_i) = 1$). The fourth time slot is the downloading time for retrieving the results from USV and satellite, denoted by $t_{j,i}^{\text{Ph-IV}}$ (in the case of $x_j(m_i) = 1$) and $\hat{t}_{k,i}^{\text{Ph-IV}}$ (in the case of $\hat{x}_k(m_i) = 1$).

For energy harvesting duration, we use η_i to denote the WPT conversion efficiency of radio frequency to direct current for UAV i. The harvested energy for UAV i in the WPT duration can be expressed as

$$E_i^{\text{H}} = \eta_i p_i^{\text{H}} \tau_i^{\text{H}}, \forall i \in \mathcal{I}, \quad (10)$$

where p_i^{H} means the transmitting power for UAV i. The maximum transmitting power is denoted by $p_{\text{H}}^{\max}$, which leads to the following constraints

$$0 \leq p_i^{\text{H}} \leq p_{\text{H}}^{\max}, \forall i \in \mathcal{I}. \quad (11)$$

We consider that UAVs equipped with solar photovoltaic (PV) panels can harvest solar energy. Let N_s denote the number of solar PV panels equipped in UAV. Within the WPT duration, the harvested solar energy of UAV i can be expressed as

$$E_i^{\text{PV}} = \varsigma \Upsilon_s N_s I_{\text{pv}}(t) \tau_i^{\text{H}}, \forall i \in \mathcal{I}, \quad (12)$$

where ς is the efficiency of solar PV panel. Υ_s means the area of solar PV panel equipped in UAV. $I_{\text{pv}}(t)$ indicates the solar irradiance at time t. Moreover, during task offloading process,

UAVs can maintain the energy harvesting from solar power in preparation for the next task offloading episode.

Phase I for local computing delay with its energy consumption: If task m_i is partially processed by UAV i, the local computing delay is expressed as $t_i^{\mathrm{Ph-I}}$. Let κ_i denote the power consumption coefficient of UAV i depending on the CPU chip architecture. We can express the energy consumption of UAV i for computing task m_i as [50]

$$E_i^{\mathrm{Ph-I}} = \kappa_i \mu_i^{\mathrm{UAV}} \left(S_{m_i}^{\mathrm{tot}} - s_{m_i}^{\mathrm{off}} \right) \left(\frac{\mu_i^{\mathrm{UAV}} \left(S_{m_i}^{\mathrm{tot}} - s_{m_i}^{\mathrm{off}} \right)}{t_i^{\mathrm{Ph-I}}} \right)^2$$

$$= \kappa_i \frac{\left(\mu_i^{\mathrm{UAV}} \right)^3 \left(S_{m_i}^{\mathrm{tot}} - s_{m_i}^{\mathrm{off}} \right)^3}{\left(t_i^{\mathrm{Ph-I}} \right)^2}, \forall i \in \mathcal{I}, \quad (13)$$

where parameter μ_i^{UAV} means the number of CPU cycles required for executing one task input-bit of UAV i.

Phase II for data uploading delay with its energy consumption: There are two choices for computing offloading, i.e., offloading to USV and offloading to LEO satellite. If task m_i is partially offloaded to USV j (i.e., $x_j(m_i) = 1$), the uploading delay can be expressed as

$$t_{i,j}^{\mathrm{Ph-II}} = \frac{s_{m_i}^{\mathrm{off}}}{r_{i,j}^{\mathrm{UAV}}}, \forall i \in \mathcal{I}, \forall j \in \mathcal{J}. \quad (14)$$

According to (9) and (14), we can obtain the required transmission power of UAV i when offloading workload to USV j as follows

$$p_{i,j}^{\mathrm{UAV}} = \frac{W_j^{\mathrm{up}} \sigma_j^2}{g_{i,j}^{\mathrm{UAV}}} \left(2^{\frac{s_{m_i}^{\mathrm{off}}}{t_{i,j}^{\mathrm{Ph-II}} W_j^{\mathrm{up}}}} - 1 \right), \forall i \in \mathcal{I}, \forall j \in \mathcal{J}. \quad (15)$$

The energy consumption of UAV i for offloading workload $s_{m_i}^{\mathrm{off}}$ to USV j can be expressed as

$$E_{i,j}^{\mathrm{Ph-II}} = p_{i,j}^{\mathrm{UAV}} t_{i,j}^{\mathrm{Ph-II}}$$

$$= \frac{t_{i,j}^{\mathrm{Ph-II}} W_j^{\mathrm{up}} \sigma_j^2}{g_{i,j}^{\mathrm{UAV}}} \left(2^{\frac{s_{m_i}^{\mathrm{off}}}{t_{i,j}^{\mathrm{Ph-II}} W_j^{\mathrm{up}}}} - 1 \right), \forall i \in \mathcal{I}, \forall j \in \mathcal{J}. \quad (16)$$

If task m_i is partially offloaded to LEO satellite (i.e., $\hat{x}_k(m_i) = 1$), the transmission delay between UAV i and satellite k can be expressed as

$$\hat{t}_{i,k}^{\mathrm{Ph-II}} = \frac{s_{m_i}^{\mathrm{off}}}{\hat{r}_{i,k}^{\mathrm{UAV}}}, \forall i \in \mathcal{I}, \forall k \in \mathcal{K}. \quad (17)$$

The required transmission power for UAV i to offload workload $s_{m_i}^{\mathrm{off}}$ can be obtained based on (6) and (17), i.e.,

$$\hat{p}_{i,k}^{\mathrm{UAV}} = \frac{\hat{W}_k^{\mathrm{up}} \sigma_k^2}{\hat{g}_{i,k}^{\mathrm{UAV}}} \left(2^{\frac{s_{m_i}^{\mathrm{off}}}{\hat{t}_{i,k}^{\mathrm{Ph-II}} \hat{W}_k^{\mathrm{up}}}} - 1 \right), \forall i \in \mathcal{I}, \forall k \in \mathcal{K}. \quad (18)$$

The energy consumption of UAV i for offloading workload $s_{m_i}^{\mathrm{off}}$ to LEO satellite k can be expressed as

$$\hat{E}_{i,k}^{\mathrm{Ph-II}} = \hat{p}_{i,k}^{\mathrm{UAV}} \hat{t}_{i,k}^{\mathrm{Ph-II}}$$

$$= \frac{\hat{t}_{i,k}^{\mathrm{Ph-II}} \hat{W}_k^{\mathrm{up}} \sigma_k^2}{\hat{g}_{i,k}^{\mathrm{UAV}}} \left(2^{\frac{s_{m_i}^{\mathrm{off}}}{\hat{t}_{i,k}^{\mathrm{Ph-II}} \hat{W}_k^{\mathrm{up}}}} - 1 \right), \forall i \in \mathcal{I}, \forall k \in \mathcal{K}. \quad (19)$$

Phase III for offloading computing delay: In the case of offloading task to USV (i.e., $x_j(m_i) = 1$), the computing delay $t_j^{\mathrm{Ph-III}}$ by USV j can be expressed as

$$t_j^{\mathrm{Ph-III}} = \rho_j^{\mathrm{USV}} \frac{s_{m_i}^{\mathrm{off}}}{\mu_j^{\mathrm{USV}}}, \forall i \in \mathcal{I}, \forall j \in \mathcal{J}, \quad (20)$$

where ρ_j^{USV} denotes the number of CPU cycles for processing one bit of data by USV j and μ_j^{USV} means the computing-rate of USV j in CPU cycles per second.

In the case of offloading task to LEO satellite (i.e., $\hat{x}_k(m_i) = 1$), the computing delay $\hat{t}_k^{\mathrm{Ph-III}}$ by satellite k can be denoted as

$$\hat{t}_k^{\mathrm{Ph-III}} = \rho_k^{\mathrm{LEO}} \frac{s_{m_i}^{\mathrm{off}}}{\mu_k^{\mathrm{LEO}}}, \forall i \in \mathcal{I}, \forall k \in \mathcal{K}. \quad (21)$$

Here, ρ_k^{LEO} denotes the number of CPU cycles for processing one bit of data by satellite k. μ_k^{LEO} expresses the computing-rate of satellite k in CPU cycles per second.

Phase IV for data downloading delay: We use a compression ratio ϵ_i to describe the relationship between UAV i's offloading workload $s_{m_i}^{\mathrm{off}}$ and the associated computing results to be transmitted from USV/satellite to UAV, i.e.,

$$s_{m_i}^{\mathrm{tran}} = \epsilon_i s_{m_i}^{\mathrm{off}}, \forall i \in \mathcal{I}, \forall m_i \in \mathcal{M}. \quad (22)$$

In the case of transmitting results from USV to UAV (i.e., $x_j(m_i) = 1$), the data downloading delay $t_{j,i}^{\mathrm{Ph-IV}}$ in Phase IV can be expressed as

$$t_{j,i}^{\mathrm{Ph-IV}} = \frac{s_{m_i}^{\mathrm{tran}}}{r_{j,i}^{\mathrm{USV}}} = \frac{\epsilon_i s_{m_i}^{\mathrm{off}}}{r_{j,i}^{\mathrm{USV}}}, \forall i \in \mathcal{I}, \forall j \in \mathcal{J}. \quad (23)$$

In (23), $r_{j,i}^{\mathrm{USV}}$ means the data transmission rate from USV j to UAV i, which can be expressed as

$$r_{j,i}^{\mathrm{USV}} = W_j^{\mathrm{do}} \log_2 \left(1 + \frac{p_{j,i}^{\mathrm{USV}} g_{j,i}^{\mathrm{USV}}}{W_j^{\mathrm{do}} \sigma_i^2} \right), \forall i \in \mathcal{I}, \forall j \in \mathcal{J}, \quad (24)$$

where W_j^{do} denotes the downlink bandwidth of USV j. $p_{j,i}^{\mathrm{USV}}$ indicates the transmission power from USV j to UAV i. $g_{j,i}^{\mathrm{USV}}$ denotes the channel gain between USV j to UAV i. σ_i^2 means the background noise power at UAV i.

In the case of transmitting results from LEO satellite to UAV (i.e., $\hat{x}_k(m_i) = 1$), we can express the data downloading delay $t_{k,i}^{\mathrm{Ph-IV}}$ in Phase IV as

$$\hat{t}_{k,i}^{\mathrm{Ph-IV}} = \frac{s_{m_i}^{\mathrm{tran}}}{r_{k,i}^{\mathrm{LEO}}} = \frac{\epsilon_i s_{m_i}^{\mathrm{off}}}{r_{k,i}^{\mathrm{LEO}}}, \forall i \in \mathcal{I}, \forall k \in \mathcal{K}, \quad (25)$$

where $r_{k,i}^{\mathrm{LEO}}$ indicates the data transmission rate from satellite k to UAV i. Let $\hat{W}_k^{\mathrm{do}}$ denote the downlink bandwidth of satellite k, use $p_{k,i}^{\mathrm{LEO}}$ to denote the transmission power from satellite k to UAV i, and use $g_{k,i}^{\mathrm{LEO}}$ to express the channel gain between

satellite k and UAV i. We can obtain

$$r_{k,i}^{\text{LEO}} = \hat{W}_k^{\text{do}} \log_2 \left(1 + \frac{p_{k,i}^{\text{LEO}} g_{k,i}^{\text{LEO}}}{\hat{W}_k^{\text{do}} \sigma_i^2} \right), \forall i \in \mathcal{I}, \forall k \in \mathcal{K}. \quad (26)$$

Based on above analysis, the overall delay for completing UAV i's workload can be expressed as

$$t_i^{\text{ove}} = \max \left\{ t_i^{\text{Ph-I}}, \left(t_{i,j}^{\text{Ph-II}} + t_j^{\text{Ph-III}} + t_{j,i}^{\text{Ph-IV}} \right) x_j(m_i), \right.$$
$$\left. \left(\hat{t}_{i,k}^{\text{Ph-II}} + \hat{t}_k^{\text{Ph-III}} + \hat{t}_{k,i}^{\text{Ph-IV}} \right) \hat{x}_k(m_i) \right\},$$
$$\forall i \in \mathcal{I}, \forall j \in \mathcal{J}, \forall k \in \mathcal{K}. \quad (27)$$

The complete cycle for the proposed multi-access computing offloading satisfies the following constraint

$$\tau_i^{\text{H}} + t_i^{\text{ove}} \leq \Gamma, \forall i \in \mathcal{I}. \quad (28)$$

According to [51], when UAV maintains the hovering status, the power consumption is affected by the blade profile power and induced power, which can be expressed as

$$p_i^{\text{hov}} = \underbrace{\frac{p^{\text{coe}}}{8} A^{\text{den}} \iota^{\text{rat}} \Omega B^3 C^3}_{\text{blade profile power}} + \underbrace{(1+F) \frac{w^{\frac{3}{2}}}{\sqrt{2 A^{\text{den}} \Omega}}}_{\text{induced power}}, \forall i \in \mathcal{I},$$
$$\quad (29)$$

where p^{coe} means the profile drag coefficient. A^{den} indicates the air density. ι^{rat} denotes the rotor solidity, which is the ratio of the total blade area to the disc area. Ω is the rotor disc area. B expresses the blade angular velocity. C means the rotor radius. w denotes the weight of UAV. F is the incremental correction factor to induced power. The energy consumption for UAV i hovering in the air can be expressed as

$$E_i^{\text{hov}} = p_i^{\text{hov}} t_i^{\text{ove}}, \forall i \in \mathcal{I}. \quad (30)$$

The overall consumed energy for completing each UAV's workload consists of the local computing energy in Phase I, the offloading energy consumption in Phase II, and the hovering energy consumption, which can be expressed as

$$E_i^{\text{ove}} = w E_i^{\text{Ph-I}} + E_{i,j}^{\text{Ph-II}} x_j(m_i) + \hat{E}_{i,k}^{\text{Ph-II}} \hat{x}_k(m_i) + E_i^{\text{hov}},$$
$$\forall i \in \mathcal{I}, \forall j \in \mathcal{J}, \forall k \in \mathcal{K}. \quad (31)$$

The consumed energy of each UAV cannot exceed its harvested energy, which leads to the following constraint

$$E_i^{\text{ove}} \leq E_i^{\text{H}} + E_i^{\text{PV}}, \forall i \in \mathcal{I}. \quad (32)$$

D. Problem Formulation

Based on the system model analysis, we aim at formulating a joint optimization problem to optimize the offloading decision, the time scheduling, and the transmitting power, with the objective of minimizing the harvested energy described in (32). This means that the harvested energy should enable all UAVs to process their tasks. We define an offloading decision matrix as $\boldsymbol{X} = \{\boldsymbol{x}; \hat{\boldsymbol{x}}\}$ in which $\boldsymbol{x} = \{x_j(m_i)\}_{\forall j \in \mathcal{J}, \forall m_i \in \mathcal{M}}$ and $\hat{\boldsymbol{x}} = \{\hat{x}_k(m_i)\}_{\forall k \in \mathcal{K}, \forall m_i \in \mathcal{M}}$. Each element in $\boldsymbol{X}$ corresponds to an offloading decision. We define a time scheduling matrix as $\boldsymbol{T} = \{t_i^{\text{Ph-I}}; t_{i,j}^{\text{Ph-II}}; \hat{t}_{i,k}^{\text{Ph-II}}; \tau_i^{\text{H}}\}_{\forall i \in \mathcal{I}, \forall j \in \mathcal{J}, \forall k \in \mathcal{K}}$ including the

local computing delay, the offloading duration, and the WPT duration. The transmitting power matrix is defined as $\boldsymbol{P} = \{p_i^{\text{H}}\}_{\forall i \in \mathcal{I}}$. The detailed problem formulation to <u>M</u>inimize the <u>C</u>umulative <u>T</u>ransmitted <u>E</u>nergy is expressed as follows

$$(\text{MCTE}): \quad \min E^{\text{tot}} = \sum_{i=1}^{I} p_i^{\text{H}} \tau_i^{\text{H}}$$

subject to : $\quad x_j(m_i), \hat{x}_k(m_i) \in \{0, 1\}, \forall m_i \in \mathcal{M},$
$$\forall j \in \mathcal{J}, \forall k \in \mathcal{K}, \quad (33)$$
$$x_j(m_i) + \hat{x}_k(m_i) = 1, \forall m_i \in \mathcal{M},$$
$$\forall k \in \mathcal{K}, \forall j \in \mathcal{J}, \quad (34)$$
$$0 \leq \hat{t}_{i,k}^{\text{Ph-II}} + \hat{t}_k^{\text{Ph-III}} + \hat{t}_{k,i}^{\text{Ph-IV}} \leq t_{i,k}^{\text{UAV}},$$
$$\text{if } \hat{x}_k(m_i) = 1, \forall i \in \mathcal{I}, \forall k \in \mathcal{K}, \forall m_i \in \mathcal{M}, \quad (35)$$
$$0 \leq s_{m_i}^{\text{off}} \leq S_{m_i}^{\text{tot}}, \forall m_i \in \mathcal{M}, \quad (36)$$
$$0 \leq p_{i,j}^{\text{UAV}} \leq p_i^{\text{UAV-max}}, \forall i \in \mathcal{I}, \forall j \in \mathcal{J}, \quad (37)$$
$$0 \leq \hat{p}_{i,k}^{\text{UAV}} \leq p_i^{\text{UAV-max}}, \forall i \in \mathcal{I}, \forall k \in \mathcal{K}, \quad (38)$$
$$0 \leq p_{j,i}^{\text{USV}} \leq p_j^{\text{USV-max}}, \forall i \in \mathcal{I}, \forall j \in \mathcal{J}, \quad (39)$$
$$0 \leq p_{k,i}^{\text{LEO}} \leq p_k^{\text{LEO-max}}, \forall i \in \mathcal{I}, \forall k \in \mathcal{K}, \quad (40)$$

constraints (11), (28), (32),

variables : $\quad \boldsymbol{X}, \boldsymbol{T}, \boldsymbol{P}.$

In the formulated Problem (MCTE), constraint (33) means the offloading decision of UAV, i.e., offloading task m_i to USVs or offloading task m_i to satellites. Constraint (34) indicates that the offloading workload cannot be processed by USV and satellite simultaneously, i.e., each task can only be processed by either a USV or a satellite. Constraint (35) ensures that if the offloading workload is processed by satellite, the uploading time, computing time, and downloading time should be within the available communication time between UAV and satellite. Constraint (36) denotes that the offloading workload of UAV cannot exceed the total workload $S_{m_i}^{\text{tot}}$. Constraints (37) and (38) guarantee that the transmission power of UAV to USV and UAV to satellite cannot exceed its maximum $p_i^{\text{UAV-max}}$. Constraint (39) guarantees that the transmission power from USV to UAV cannot exceed USV's maximum $p_j^{\text{USV-max}}$. Constraint (40) ensures that the transmission power for sending the results to UAV cannot exceed satellite's maximum $p_k^{\text{LEO-max}}$. Problem (MCTE) is a mixed-integer and multi-objective combinatorial optimization problem, which is hard to solve. In the next section, we will propose algorithms to obtain the solutions.

IV. PROPOSED ALGORITHMS TO SOLVE THE FORMULATED PROBLEM

In this section, we first decompose the formulated problem and obtain an equivalent problem. Next, we propose efficient algorithms to solve the formulated problem.

A. Problem Transformation

We first determine the local computing duration by UAVs. Let $\mu_i^{\max}$ denote the maximum computing-rate of UAV i. The local computing delay will be at least $\rho_i^{\mathrm{UAV}}\frac{S_{m_i}^{\mathrm{tot}}-s_{m_i}^{\mathrm{off}}}{\mu_i^{\max}}$, where ρ_i^{UAV} is the computing-rate of UAV i in CPU cycles per second. As such, we can express the local computing time constraint as

$$t_i^{\min} \leq t_i^{\mathrm{Ph-I}} \leq t_i^{\max}, \forall i \in \mathcal{I}, \tag{41}$$

where $t_i^{\max} = \Gamma$ and $t_i^{\min} = \rho_i^{\mathrm{UAV}}\frac{S_{m_i}^{\mathrm{tot}}-s_{m_i}^{\mathrm{off}}}{\mu_i^{\max}}$.

In the following, we determine the constraint for offloading computing duration based on their maximum transmission power. Based on (14), the data uploading delay from UAV to USV in Phase II satisfies the following constraint

$$t_{i,j}^{\mathrm{UAV-min}} \leq t_{i,j}^{\mathrm{Ph-II}} \leq t_{i,j}^{\mathrm{UAV-max}}, \forall i \in \mathcal{I}, \forall j \in \mathcal{J}. \tag{42}$$

In (42), $t_{i,j}^{\mathrm{UAV-max}} = x_j(m_i)\Gamma$ means that the maximum transmission duration cannot exceed the episode length Γ if UAV selects to offload workload to USV j, i.e., $x_j(m_i) = 1$. The minimum transmission time is expressed as $t_{i,j}^{\mathrm{UAV-min}} = x_j(m_i)\frac{s_{m_i}^{\mathrm{off}}}{W_j^{\mathrm{up}}\log_2\left(1+\frac{p_i^{\mathrm{UAV-max}}g_{i,j}^{\mathrm{UAV}}}{W_j^{\mathrm{up}}\sigma_j^2}\right)}$ based on the maximum transmission power. Based on constraints (32) and (42), we can derive that there is a tradeoff between the energy consumption and the data uploading delay when offloading task to USV in Phase II.

Similarly, the above analysis is also held for data uploading delay $\hat{t}_{i,k}^{\mathrm{Ph-II}}$ to satellite. We have the following constraint

$$\hat{t}_{i,k}^{\mathrm{UAV-min}} \leq \hat{t}_{i,k}^{\mathrm{Ph-II}} \leq \hat{t}_{i,k}^{\mathrm{UAV-max}}, \forall i \in \mathcal{I}, \forall k \in \mathcal{K}. \tag{43}$$

Here, $t_{i,k}^{\mathrm{UAV-max}} = \hat{x}_k(m_i)\Gamma$ denotes that the maximum transmission duration cannot exceed the episode length Γ if UAV selects to offload workload to satellite k, i.e., $\hat{x}_k(m_i) = 1$. The minimum transmission delay is obtained by $t_{i,k}^{\mathrm{UAV-min}} = \hat{x}_k(m_i)\frac{s_{m_i}^{\mathrm{off}}}{\hat{W}_k^{\mathrm{up}}\log_2\left(1+\frac{p_i^{\mathrm{UAV-max}}\hat{g}_{i,k}^{\mathrm{UAV}}}{\hat{W}_k^{\mathrm{up}}\sigma_k^2}\right)}$. Constraints (32) and (43) address the tradeoff between the energy consumption and data uploading delay when offloading task to satellite in Phase II.

In data downloading phase from USV to UAV, the delay $t_{j,i}^{\mathrm{Ph-IV}}$ satisfies

$$t_{j,i}^{\mathrm{USV-min}} \leq t_{j,i}^{\mathrm{Ph-IV}} \leq t_{j,i}^{\mathrm{USV-max}}, \forall i \in \mathcal{I}, \forall j \in \mathcal{J}, \tag{44}$$

where $t_{j,i}^{\mathrm{USV-max}} = x_j(m_i)\Gamma$ and $t_{j,i}^{\mathrm{USV-min}} = x_j(m_i)\frac{\epsilon_i s_{m_i}^{\mathrm{off}}}{W_j^{\mathrm{do}}\log_2(1+\frac{p_j^{\mathrm{USV-max}}g_{j,i}^{\mathrm{USV}}}{W_j^{\mathrm{do}}\sigma_i^2})}$.

In data downloading phase from satellite to UAV, we can express the constraint for delay $\hat{t}_{k,i}^{\mathrm{Ph-IV}}$ as

$$\hat{t}_{k,i}^{\mathrm{LEO-min}} \leq \hat{t}_{k,i}^{\mathrm{Ph-IV}} \leq \hat{t}_{k,i}^{\mathrm{LEO-max}}, \forall i \in \mathcal{I}, \forall k \in \mathcal{K}, \tag{45}$$

where $\hat{t}_{k,i}^{\mathrm{LEO-max}} = \hat{x}_k(m_i)\Gamma$ and $\hat{t}_{k,i}^{\mathrm{LEO-min}} = \hat{x}_k(m_i)\frac{\epsilon_i s_{m_i}^{\mathrm{off}}}{\hat{W}_k^{\mathrm{do}}\log_2\left(1+\frac{p_k^{\mathrm{LEO-max}}g_{k,i}^{\mathrm{LEO}}}{\hat{W}_k^{\mathrm{do}}\sigma_i^2}\right)}$.

Based on the above analysis, we propose a vertical decomposition method to derive an equivalent optimization problem.
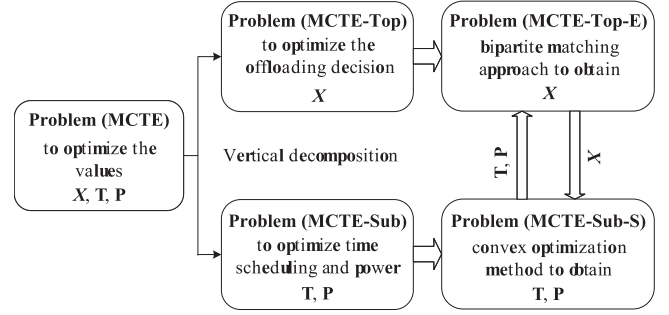

Fig. 4. The vertical architecture for solving Problem (MCTE).

Problem (MCTE) is decomposed into a top-problem and a sub-problem. The decomposition framework for solving the formulated Problem (MCTE) is depicted in Fig. 4.

- In the sub-problem, we give the values of $\boldsymbol{x} = \{x_j(m_i)\}_{\forall j \in \mathcal{J}, \forall m_i \in \mathcal{M}}$ and $\hat{\boldsymbol{x}} = \{\hat{x}_k(m_i)\}_{\forall k \in \mathcal{K}, \forall m_i \in \mathcal{M}}$ to minimize the cumulative transmitted energy by optimizing the time scheduling $\boldsymbol{T}$ and the transmitting power $\boldsymbol{P}$. Sub-problem is expressed as

$$(\mathrm{MCTE-Sub}): \min E_{\mathrm{sub}}^{\mathrm{tot}} = \sum_{i=1}^{I} p_i^{\mathrm{H}}\tau_i^{\mathrm{H}}$$

$$\text{subject to}: \text{constraints (11), (28), (32), (36)–(35),}$$

$$\text{constraints (41)–(45),}$$

$$\text{variables}: \boldsymbol{T}, \boldsymbol{P}.$$

- Based on the obtained values of time scheduling $\boldsymbol{T}$ and transmitting power $\boldsymbol{P}$, Top-problem can further optimize the offloading decision $\boldsymbol{X}$ to minimize the cumulative transmitted energy. We express the Top-problem as

$$(\mathrm{MCTE-Top}): \min E_{\mathrm{top}}^{\mathrm{tot}} = \sum_{i=1}^{I} p_i^{\mathrm{H}}\tau_i^{\mathrm{H}}$$

$$\text{subject to}: \text{constraints (33)–(35),}$$

$$\text{variables}: \boldsymbol{X}.$$

B. Proposed Algorithms to Solve Problem (MCTE-Sub)

Proposition 1: Given the values of $\{x_j(m_i)\}_{\forall j \in \mathcal{J}, \forall m_i \in \mathcal{M}}$ and $\{\hat{x}_k(m_i)\}_{\forall k \in \mathcal{K}, \forall m_i \in \mathcal{M}}$, Problem (MCTE-Sub) is a strictly convex optimization problem.

Proof: For the given values of $\{x_j(m_i)\}_{\forall j \in \mathcal{J}, \forall m_i \in \mathcal{M}}$ and $\{\hat{x}_k(m_i)\}_{\forall k \in \mathcal{K}, \forall m_i \in \mathcal{M}}$, it can be observed that constraints (11), (36)–(45) are within the closed intervals, which correspond to the convex sets. We begin proving the convexity of constraint (32). Constraint (32) can be rewritten as

$$\frac{t_{i,j}^{\mathrm{Ph-II}}W_j^{\mathrm{up}}\sigma_j^2}{g_{i,j}^{\mathrm{UAV}}}\left(2^{\frac{s_{m_i}^{\mathrm{off}}}{t_{i,j}^{\mathrm{Ph-II}}W_j^{\mathrm{up}}}} - 1\right)x_j(m_i)$$

$$+ \frac{\hat{t}_{i,k}^{\mathrm{Ph-II}}\hat{W}_k^{\mathrm{up}}\sigma_k^2}{\hat{g}_{i,k}^{\mathrm{UAV}}}\left(2^{\frac{s_{m_i}^{\mathrm{off}}}{\hat{t}_{i,k}^{\mathrm{Ph-II}}\hat{W}_k^{\mathrm{up}}}} - 1\right)\hat{x}_k(m_i) + p_i^{\mathrm{hov}}t_i^{\mathrm{ove}}$$

$$+ \kappa_i \frac{\left(\mu_i^{\mathrm{UAV}}\right)^3 \left(S_{m_i}^{\mathrm{tot}} - s_{m_i}^{\mathrm{off}}\right)^3}{\left(t_i^{\mathrm{Ph-I}}\right)^2} - \eta_i p_i^{\mathrm{H}} \tau_i^{\mathrm{H}} - \varsigma \Upsilon_s N_s I_{\mathrm{pv}}(t) \tau_i^{\mathrm{H}} \leq 0.$$

$$(46)$$

Since the offloading workload cannot be executed simultaneously by USV and satellite, i.e., $x_j(m_i)$ and $\hat{x}_k(m_i)$ cannot be equal to one at the same time, constraint (46) can be divided into two cases. We use $F^{\mathrm{case-1}}(t_i^{\mathrm{Ph-I}}, t_{i,j}^{\mathrm{Ph-II}}, p_i^{\mathrm{H}}, \tau_i^{\mathrm{H}})$ and $F^{\mathrm{case-2}}(t_i^{\mathrm{Ph-I}}, \hat{t}_{i,k}^{\mathrm{Ph-II}}, p_i^{\mathrm{H}}, \tau_i^{\mathrm{H}})$ to denote the left-hand side of constraint (46) with respect to $t_i^{\mathrm{Ph-I}}$, $t_{i,j}^{\mathrm{Ph-II}}$, $\hat{t}_{i,k}^{\mathrm{Ph-II}}$, p_i^{H} and τ_i^{H}. We can express the two cases as

$$\begin{cases} F^{\mathrm{case-1}}\left(t_i^{\mathrm{Ph-I}}, t_{i,j}^{\mathrm{Ph-II}}, p_i^{\mathrm{H}}, \tau_i^{\mathrm{H}}\right) = \kappa_i \frac{\left(\mu_i^{\mathrm{UAV}}\right)^3 \left(S_{m_i}^{\mathrm{tot}} - s_{m_i}^{\mathrm{off}}\right)^3}{\left(t_i^{\mathrm{Ph-I}}\right)^2} \\ + \frac{t_{i,j}^{\mathrm{Ph-II}} W_j^{\mathrm{up}} \sigma_j^2}{g_{i,j}^{\mathrm{UAV}}} \left(2^{\frac{s_{m_i}^{\mathrm{off}}}{t_{i,j}^{\mathrm{Ph-II}} W_j^{\mathrm{up}}}} - 1\right) + p_i^{\mathrm{hov}} t_i^{\mathrm{ove}} \\ - \eta_i p_i^{\mathrm{H}} \tau_i^{\mathrm{H}} - \varsigma \Upsilon_s N_s I_{\mathrm{pv}}(t) \tau_i^{\mathrm{H}}, \\ F^{\mathrm{case-2}}\left(t_i^{\mathrm{Ph-I}}, \hat{t}_{i,k}^{\mathrm{Ph-II}}, p_i^{\mathrm{H}}, \tau_i^{\mathrm{H}}\right) = \kappa_i \frac{\left(\mu_i^{\mathrm{UAV}}\right)^3 \left(S_{m_i}^{\mathrm{tot}} - s_{m_i}^{\mathrm{off}}\right)^3}{\left(t_i^{\mathrm{Ph-I}}\right)^2} \\ + \frac{\hat{t}_{i,k}^{\mathrm{Ph-II}} \hat{W}_k^{\mathrm{up}} \sigma_k^2}{\hat{g}_{i,k}^{\mathrm{UAV}}} \left(2^{\frac{s_{m_i}^{\mathrm{off}}}{\hat{t}_{i,k}^{\mathrm{Ph-II}} \hat{W}_k^{\mathrm{up}}}} - 1\right) + p_i^{\mathrm{hov}} t_i^{\mathrm{ove}} \\ - \eta_i p_i^{\mathrm{H}} \tau_i^{\mathrm{H}} - \varsigma \Upsilon_s N_s I_{\mathrm{pv}}(t) \tau_i^{\mathrm{H}}. \end{cases}$$

$$(47)$$

Here, we find that $F^{\mathrm{case-1}}(t_i^{\mathrm{Ph-I}}, t_{i,j}^{\mathrm{Ph-II}}, p_i^{\mathrm{H}}, \tau_i^{\mathrm{H}})$ and $F^{\mathrm{case-2}}(t_i^{\mathrm{Ph-I}}, \hat{t}_{i,k}^{\mathrm{Ph-II}}, p_i^{\mathrm{H}}, \tau_i^{\mathrm{H}})$ are continuous and differentiable with respect to $t_i^{\mathrm{Ph-I}}$, $t_{i,j}^{\mathrm{Ph-II}}$, $\hat{t}_{i,k}^{\mathrm{Ph-II}}$, p_i^{H} and τ_i^{H}. The Hessian matrix of $F^{\mathrm{case-1}}(t_i^{\mathrm{Ph-I}}, t_{i,j}^{\mathrm{Ph-II}}, p_i^{\mathrm{H}}, \tau_i^{\mathrm{H}})$ can be expressed as

$$\nabla^2 F^{\mathrm{case-1}}$$

$$= \begin{bmatrix} \frac{\left(s_{m_i}^{\mathrm{off}}\right)^2 \sigma_j^2 (\ln 2)^2}{W_j^{\mathrm{up}} g_{i,j}^{\mathrm{UAV}} \left(t_{i,j}^{\mathrm{Ph-II}}\right)^3} 2^{\frac{s_{m_i}^{\mathrm{off}}}{t_{i,j}^{\mathrm{Ph-II}} W_j^{\mathrm{up}}}} & 0 & 0 & 0 \\ 0 & \frac{6\kappa_i \left(\mu_i^{\mathrm{UAV}}\right)^3 \left(S_{m_i}^{\mathrm{tot}} - s_{m_i}^{\mathrm{off}}\right)^3}{\left(t_i^{\mathrm{Ph-I}}\right)^4} & 0 & 0 \\ 0 & 0 & 0 & 0 \\ 0 & 0 & 0 & 0 \end{bmatrix}.$$

$$(48)$$

It can be found that the matrix in (48) is a diagonal with non-negative elements. As such, the Hessian matrix is a positive semidefinite, with the result that the multi-variable function $F^{\mathrm{case-1}}(t_i^{\mathrm{Ph-I}}, t_{i,j}^{\mathrm{Ph-II}}, p_i^{\mathrm{H}}, \tau_i^{\mathrm{H}})$ is convex. Similarly, the Hessian matrix of $F^{\mathrm{case-2}}(t_i^{\mathrm{Ph-I}}, \hat{t}_{i,k}^{\mathrm{Ph-II}}, p_i^{\mathrm{H}}, \tau_i^{\mathrm{H}})$ can be expressed as

$$\nabla^2 F^{\mathrm{case-2}}$$

$$= \begin{bmatrix} \frac{\left(s_{m_i}^{\mathrm{off}}\right)^2 \sigma_k^2 (\ln 2)^2}{\hat{W}_k^{\mathrm{up}} \hat{g}_{i,k}^{\mathrm{UAV}} \left(\hat{t}_{i,k}^{\mathrm{Ph-II}}\right)^3} 2^{\frac{s_{m_i}^{\mathrm{off}}}{\hat{t}_{i,k}^{\mathrm{Ph-II}} \hat{W}_k^{\mathrm{up}}}} & 0 & 0 & 0 \\ 0 & \frac{6\kappa_i \left(\mu_i^{\mathrm{UAV}}\right)^3 \left(S_{m_i}^{\mathrm{tot}} - s_{m_i}^{\mathrm{off}}\right)^3}{\left(t_i^{\mathrm{Ph-I}}\right)^4} & 0 & 0 \\ 0 & 0 & 0 & 0 \\ 0 & 0 & 0 & 0 \end{bmatrix}.$$

$$(49)$$

We can observe the same results by analyzing the Hessian matrix of $F^{\mathrm{case-2}}(t_i^{\mathrm{Ph-I}}, \hat{t}_{i,k}^{\mathrm{Ph-II}}, p_i^{\mathrm{H}}, \tau_i^{\mathrm{H}})$ in Case 2. Therefore, constraint (32) is a convex set. Problem (MCTE-Sub) is a strictly convex optimization problem. This completes our proof. ∎

In the following, we decompose Problem (MCTE-Sub) into a separated problem for each UAV. The following propositions are given to simplify Problem (MCTE-Sub).

Proposition 2: The data downloading delay in Phase IV is determined by $t_{j,i}^{\mathrm{Ph-IV*}}$ when UAVs offload task to USVs, i.e.,

$$t_{j,i}^{\mathrm{Ph-IV*}} = t_{j,i}^{\mathrm{USV-min}}, \forall i \in \mathcal{I}, \forall j \in \mathcal{J}. \quad (50)$$

When UAVs offload task to satellites, the data downloading delay $\hat{t}_{k,i}^{\mathrm{Ph-IV*}}$ in Phase IV is determined by

$$\hat{t}_{k,i}^{\mathrm{Ph-IV*}} = \hat{t}_{k,i}^{\mathrm{LEO-min}}, \forall i \in \mathcal{I}, \forall k \in \mathcal{K}. \quad (51)$$

Proof: The value of $t_{j,i}^{\mathrm{Ph-IV}}$ is constrained by (28) and (44). Considering that (28) is a strictly time constraint, to meet the time scheduling requirement, it is desirable for $t_{j,i}^{\mathrm{Ph-IV}}$ to take the minimum value dictated by constraint (44). As such, (50) eliminates constraint (44). Similarly, the optimal value of $\hat{t}_{k,i}^{\mathrm{Ph-IV}}$ is obtained at the minimum point dictated by constraint (45), which thus eliminates constraint (45). Therefore, (50) and (51) can be achieved at the optimal point of Problem (MCTE-Sub). ∎

Proposition 3: The harvested energy for each UAV in each episode will be

$$\Phi_i^{\mathrm{H}} = \max_{\forall i \in \mathcal{I}}$$

$$\left\{ \begin{array}{l} \frac{t_{i,j}^{\mathrm{Ph-II}} W_j^{\mathrm{up}} \sigma_j^2}{\eta_i g_{i,j}^{\mathrm{UAV}}} \left(2^{\frac{s_{m_i}^{\mathrm{off}}}{t_{i,j}^{\mathrm{Ph-II}} W_j^{\mathrm{up}}}} - 1\right) x_j(m_i) \\ + \frac{\hat{t}_{i,k}^{\mathrm{Ph-II}} \hat{W}_k^{\mathrm{up}} \sigma_k^2}{\eta_i \hat{g}_{i,k}^{\mathrm{UAV}}} \left(2^{\frac{s_{m_i}^{\mathrm{off}}}{\hat{t}_{i,k}^{\mathrm{Ph-II}} \hat{W}_k^{\mathrm{up}}}} - 1\right) \hat{x}_k(m_i) \\ + \kappa_i \frac{\left(\mu_i^{\mathrm{UAV}}\right)^3 \left(S_{m_i}^{\mathrm{tot}} - s_{m_i}^{\mathrm{off}}\right)^3}{\left(t_i^{\mathrm{Ph-I}}\right)^2 \eta_i} + \frac{p_i^{\mathrm{hov}} t_i^{\mathrm{ove}}}{\eta_i} - \frac{\varsigma \Upsilon_s N_s I_{\mathrm{PV}}(t) \tau_i^{\mathrm{H}}}{\eta_i} \end{array} \right\}.$$

$$(52)$$

Proof: It is noticed that the objective of Problem (MCTE-Sub) is to minimize the transmitted energy. Based on constraint (32), the harvested energy Φ_i^{H} should satisfy UAV's requirement for hovering and task offloading. As such, the harvested energy for each UAV is the maximum value, with the result that constraint (32) can be eliminated by (52). ∎

For ease of expression, we introduce three functions $f_1(t_i^{\mathrm{Ph-I}})$, $f_2(t_{i,j}^{\mathrm{Ph-II}})$ and $f_3(\hat{t}_{i,k}^{\mathrm{Ph-II}})$ with respect to $t_i^{\mathrm{Ph-I}}$,

$t_{i,j}^{\text{Ph-II}}$ and $\hat{t}_{i,k}^{\text{Ph-II}}$, denoted as

$$
\begin{cases}
f_1\left(t_i^{\text{Ph-I}}\right) = \kappa_i \dfrac{\left(\mu_i^{\text{UAV}}\right)^3 \left(S_{m_i}^{\text{tot}} - s_{m_i}^{\text{off}}\right)^3}{\left(t_i^{\text{Ph-I}}\right)^2 \eta_i}, \\[4mm]
f_2\left(t_{i,j}^{\text{Ph-II}}\right) = \dfrac{t_{i,j}^{\text{Ph-II}} W_j^{\text{up}} \sigma_j^2}{\eta_i g_{i,j}^{\text{UAV}}} \left(2^{\frac{s_{m_i}^{\text{off}}}{t_{i,j}^{\text{Ph-II}} W_j^{\text{up}}}} - 1\right) x_j\left(m_i\right), \\[4mm]
f_3\left(\hat{t}_{i,k}^{\text{Ph-II}}\right) = \dfrac{\hat{t}_{i,k}^{\text{Ph-II}} \hat{W}_k^{\text{up}} \sigma_k^2}{\eta_i \hat{g}_{i,k}^{\text{UAV}}} \left(2^{\frac{s_{m_i}^{\text{off}}}{\hat{t}_{i,k}^{\text{Ph-II}} \hat{W}_k^{\text{up}}}} - 1\right) \hat{x}_k\left(m_i\right), \\[4mm]
f_4\left(t_i^{\text{Ph-I}}, t_{i,j}^{\text{Ph-II}}, \hat{t}_{i,k}^{\text{Ph-II}}\right) = \dfrac{p^{\text{hov}} t^{\text{ove}}}{\eta_i} - \dfrac{\varsigma \Upsilon_s N_s I_{\text{PV}}(t) \tau_i^{\text{H}}}{\eta_i}.
\end{cases}
\tag{53}
$$

As different UAVs may require different amounts of power for completing their workloads, it is desirable to determine different values of p_i^{H}.

Proposition 4: The total energy consumption and the harvested energy of each UAV satisfy the following equation

$$
\begin{aligned}
& f_1\left(t_i^{\text{Ph-I}}\right) + f_2\left(t_{i,j}^{\text{Ph-II}}\right) + f_3\left(\hat{t}_{i,k}^{\text{Ph-II}}\right) \\
& + f_4\left(t_i^{\text{Ph-I}}, t_{i,j}^{\text{Ph-II}}, \hat{t}_{i,k}^{\text{Ph-II}}\right) \\
& = p_i^{\text{H}} \tau_i^{\text{H}}, \forall i \in \mathcal{I}, \forall j \in \mathcal{J}, \forall k \in \mathcal{K}.
\end{aligned}
\tag{54}
$$

Proof: The left side of (54), i.e., $f_1(t_i^{\text{Ph-I}}) + f_2(t_{i,j}^{\text{Ph-II}}) + f_3(\hat{t}_{i,k}^{\text{Ph-II}}) + f_4(t_i^{\text{Ph-I}}, t_{i,j}^{\text{Ph-II}}, \hat{t}_{i,k}^{\text{Ph-II}})$ indicates the total energy consumption for completing UAV i's workload, while the right side of (54) means the harvested energy for each UAV. At the optimal point of Problem (MCTE-Sub), the total energy consumption cannot exceed the harvested energy, with the result that equality (54) holds. ∎

Through the above transformation, we can obtain an equivalent form of Problem (MCTE-Sub) as follows:

$$(\text{MCTE} - \text{Sub} - \text{E}):$$

$$
\begin{aligned}
\min E_{\text{sub-E}}^{\text{tot}} = \sum_{i=1}^{I} & f_1\left(t_i^{\text{Ph-I}}\right) + f_2\left(t_{i,j}^{\text{Ph-II}}\right) \\
& + f_3\left(\hat{t}_{i,k}^{\text{Ph-II}}\right) + f_4\left(t_i^{\text{Ph-I}}, t_{i,j}^{\text{Ph-II}}, \hat{t}_{i,k}^{\text{Ph-II}}\right)
\end{aligned}
$$

subject to : constraints (11), (28), (41)–(43), (54),

variables : $\boldsymbol{T}, \boldsymbol{P}$.

In Problem (MCTE-Sub-E), it can be identified that the objective function is separable. The harvested energy $p_i^{\text{H}} \tau_i^{\text{H}}$ for each UAV is independent from others. As a result, Problem (MCTE-Sub-E) can be further decomposed. The optimal solutions can be individually solved for each UAV under the given values of $\{x_j(m_i)\}_{\forall j \in \mathcal{J}, \forall m_i \in \mathcal{M}}$ and $\{\hat{x}_k(m_i)\}_{\forall k \in \mathcal{K}, \forall m_i \in \mathcal{M}}$. The decomposed problem is described as follows

$$(\text{MCTE} - \text{Sub} - \text{S}):$$

$$
\begin{aligned}
\min E_{\text{sub-S}}^{\text{tot}} = & f_1\left(t_i^{\text{Ph-I}}\right) + f_2\left(t_{i,j}^{\text{Ph-II}}\right) \\
& + f_3\left(\hat{t}_{i,k}^{\text{Ph-II}}\right) + f_4\left(t_i^{\text{Ph-I}}, t_{i,j}^{\text{Ph-II}}, \hat{t}_{i,k}^{\text{Ph-II}}\right)
\end{aligned}
$$

subject to : constraints (11), (28), (41)–(43), (54)

variables : $t_i^{\text{Ph-I}}, t_{i,j}^{\text{Ph-II}}, \hat{t}_{i,k}^{\text{Ph-II}}, p_i^{\text{H}}, \tau_i^{\text{H}}, \forall i \in \mathcal{I}, \forall j \in \mathcal{J},$

$$\forall k \in \mathcal{K}.$$

Problem (MCTE-Sub-S) is a convex optimization problem. The proof is similar to the analysis of Proposition 1. The solutions can be derived using the sequential quadratic programming method.

C. Proposed Algorithms to Solve Problem (MCTE-Top)

To determine the offloading decision, we adopt the bipartite matching approach to solve Problem (MCTE-Top). In the formulated bipartite graph, UAVs are connected to USVs/satellites via edges. Each edge in the graph is associated with a weight which indicates the energy consumption for completing the workload. As such, a set of edges associated with a feasible resource allocation is recorded as a matching [52], [53]. Each task of UAV is matched with a computing resource consisting of USVs and satellites.[1] For each matching, the binary variables $x_j(m_i)$ and $\hat{x}_k(m_i)$ are determined, e.g., matching task m_i with USV will result in $x_j(m_i) = 1$; matching task m_i with satellite will result in $\hat{x}_k(m_i) = 1$. The objective of the proposed matching is to find the minimum weighted graph matching (i.e., the minimum energy consumption). We introduce the concept of virtual resource by splitting the resources of satellite and USV into multiple sub-virtual resources. In the following, we present algorithms to solve Problem (MCTE-Top) using the above mentioned minimum weighted graph matching. Let $\mathcal{G} = (\mathcal{M}, \mathcal{L}, \mathcal{E}, \boldsymbol{W})$ denote the bipartite graph, where $\mathcal{M}$ indicates the set of tasks of UAVs. $\mathcal{L}$ represents the set of resources provided by UAVs, USVs and satellites. $\mathcal{E}$ means the set of all edges of the constructed bipartite graph. $\boldsymbol{W}$ denotes the weight matrix of the feasible edges. We use $\mathcal{F}$ to express a matching, and use (m_i, ℓ_{m_i}) to denote the edge that connects task m_i of UAV i with resource ℓ_{m_i}, and use $w(m_i, \ell_{m_i})$ to denote the weight of edge (m_i, ℓ_{m_i}), where $m_i \in \mathcal{M}, \ell_{m_i} = (x_j(m_i), \hat{x}_k(m_i)) \in \boldsymbol{X}$. The feasible edge in the graph can be determined based on constraints (41), (42) and (43), i.e., $t_i^{\min} \leq t_i^{\max}$, $t_{i,j}^{\text{UAV-min}} \leq t_{i,j}^{\text{UAV-max}}$ and $\hat{t}_{i,k}^{\text{UAV-min}} \leq \hat{t}_{i,k}^{\text{UAV-max}}$.

Under a given matching $\mathcal{F}$, for each edge $(m_i, \ell_{m_i}) \in \mathcal{F}$, the weight is set to $\gamma(t_i^{\text{Ph-I}}, t_{i,j}^{\text{Ph-II}}, \hat{t}_{i,k}^{\text{Ph-II}}) = f_1(t_i^{\text{Ph-I}}) + f_2(t_{i,j}^{\text{Ph-II}}) + f_3(\hat{t}_{i,k}^{\text{Ph-II}}) + f_4(t_i^{\text{Ph-I}}, t_{i,j}^{\text{Ph-II}}, \hat{t}_{i,k}^{\text{Ph-II}})$. Next, we show that the minimum weight of the cumulative transmitted energy is equal to the summation of the weights of all edges in the graph matching. As such, we can reformulate Problem (MCTE-Top) to obtain an equivalent form as follows

$$(\text{MCTE} - \text{Top} - \text{E}): \min \text{E}_{\text{top}}^{\text{tot}}$$

$$
= \sum_{(m_i, \ell_{m_i}) \in \mathcal{F}} \begin{cases} f_1\left(t_i^{\text{Ph-I}}\right) + f_2\left(t_{i,j}^{\text{Ph-II}}\right) \\ + f_3\left(\hat{t}_{i,k}^{\text{Ph-II}}\right) \\ + f_4\left(t_i^{\text{Ph-I}}, t_{i,j}^{\text{Ph-II}}, \hat{t}_{i,k}^{\text{Ph-II}}\right) \end{cases}
$$

subject to : constraints (33)–(35),

variables : $\boldsymbol{X}$.

---

[1] It is noticed that a task of UAV can only be matched with its resource or USV/satellite resources, not with other UAVs.

The objective function is defined as follows

$$\sum_{(m_i, \ell_{m_i}) \in \mathcal{F}} \left\{ \begin{array}{l} f_1\left(t_i^{\text{Ph-I}}\right) + f_2\left(t_{i,j}^{\text{Ph-II}}\right) + f_3\left(\hat{t}_{i,k}^{\text{Ph-II}}\right) \\ + f_4\left(t_i^{\text{Ph-I}}, t_{i,j}^{\text{Ph-II}}, \hat{t}_{i,k}^{\text{Ph-II}}\right) \end{array} \right\}$$

$$= \sum_{(m_i, \ell_{m_i}) \in \mathcal{F}} \gamma\left(t_i^{\text{Ph-I}}, t_{i,j}^{\text{Ph-II}}, \hat{t}_{i,k}^{\text{Ph-II}}\right). \quad (55)$$

It can be identified that the objective function of Problem (MCTE-Top-E) is to minimize the summation of the weights of all edges. Moreover, the optimal time scheduling and transmitting power are independent from others under a given matching $(m_i, \ell_{m_i}) \in \mathcal{F}$. Therefore, given a matching $\mathcal{F}$, for each edge $(m_i, \ell_{m_i}) \in \mathcal{F}$, the optimal solutions for time scheduling and transmitting power, denoted by $t_i^{\text{Ph-I},*}$, $t_{i,j}^{\text{Ph-II},*}$, $\hat{t}_{i,k}^{\text{Ph-II},*}$, $p_i^{\text{H},*}$, $\tau_i^{\text{H},*}$, can be derived by solving Problem (MCTE-Sub-S). We define the optimal value of Problem (MCTE-Sub-S) for edge (m_i, ℓ_{m_i}) as $\gamma(t_i^{\text{Ph-I},*}, t_{i,j}^{\text{Ph-II},*}, \hat{t}_{i,k}^{\text{Ph-II},*})$. Therefore, given the matching $\mathcal{F}$, the optimal value of Problem (MCTE-Top-E) can be expressed as

$$\sum_{(m_i, \ell_{m_i}) \in \mathcal{F}} \gamma\left(t_i^{\text{Ph-I},*}, t_{i,j}^{\text{Ph-II},*}, \hat{t}_{i,k}^{\text{Ph-II},*}\right). \quad (56)$$

Recall that for each edge $(m_i, \ell_{m_i}) \in \mathcal{F}$, the weight is $w(m_i, \ell_{m_i}) = \gamma(t_i^{\text{Ph-I},*}, t_{i,j}^{\text{Ph-II},*}, \hat{t}_{i,k}^{\text{Ph-II},*})$. To this end, the optimal value of Problem (MCTE-Top-E) can also be denoted as $\sum_{(m_i, \ell_{m_i}) \in \mathcal{F}} w(m_i, \ell_{m_i})$, which means the summation of the weights of all edges in matching $\mathcal{F}$. Therefore, the minimum weight of the cumulative transmitted energy is equivalent to the minimum summation of the weights of all edges. The minimum weighted matching for Problem (MCTE-Top-E) can be derived by

$$\mathcal{F}^* = \underset{\mathcal{F} \subseteq \mathcal{E}}{\arg\min} \sum_{(m_i, \ell_{m_i}) \in \mathcal{F}} w(m_i, \ell_{m_i}). \quad (57)$$

Based on the minimum weighted graph matching, we propose a parallel algorithm to solve Problem (MCTE-Top). The parallel algorithm consists of two phases: the first phase is to calculate the weights of all possible edges in parallel. We regard this phase as graph edge weight calculation (GEWC) scheme, which yields the virtual matching weights. The second stage is to determine the optimal matching for offloading decision, time scheduling and transmission power, named minimum weight graph matching (MWGM) scheme. Note that the resource allocation process can be executed simultaneously in GEWC scheme. Then, MWGM scheme intends to find the optimal matching based on the obtained weights, and it finally outputs the optimal resource allocation.

The details of the proposed algorithm for obtaining the virtual resource allocation are presented in Algorithm 1. Let $\boldsymbol{R}^{\text{vir}} = \{r_j^{\text{vir}}, r_k^{\text{vir}}\}, \forall j \in \mathcal{J}, \forall k \in \mathcal{K}$ denote the set of virtual computing resources. We define a matrix $\boldsymbol{W}^{\text{vir}} = \{w_{m_i, \ell_{m_i}}^{\text{vir}}\}^{|\mathcal{M}| \times |\boldsymbol{R}^{\text{vir}}|}$ to indicate the edge weight of each matching. We also define matrices $\boldsymbol{T}^{\text{vir}} = \{t_i^{\text{Ph-I,vir}}, t_{i,j}^{\text{Ph-II,vir}}, \hat{t}_{i,k}^{\text{Ph-II,vir}}\}, \forall i \in \mathcal{I}, \forall j \in \mathcal{J}, \forall k \in \mathcal{K}$ and $\boldsymbol{P}^{\text{vir}} = \{p_i^{\text{H,vir}}\}, \forall i \in \mathcal{I}$ to store the

---

Algorithm 1: Proposed Algorithm for Obtaining Virtual Resource Allocation.

1: **Input:** $\mathcal{I}, \mathcal{J}, \mathcal{K}, \mathcal{M}, \Gamma, S_{m_i}^{\text{tot}}, \rho_j^{\text{USV}}, \rho_k^{\text{LEO}}, \mu_j^{\text{USV}}, \mu_k^{\text{LEO}}, \mu^{\max}, p_i^{\text{UAV-max}}, p_j^{\text{USV-max}}, p_k^{\text{LEO-max}}, W_j^{\text{up}}, \hat{W}_k^{\text{up}}, W_j^{\text{do}}, \hat{W}_k^{\text{do}}, g_{i,j}^{\text{UAV}}, g_{j,i}^{\text{USV}}, \hat{g}_{i,k}^{\text{UAV}}, g_{k,i}^{\text{LEO}}, \forall i, j, k.$

2: **Initialization:** initialize $\boldsymbol{R}^{\text{vir}} = \emptyset, \boldsymbol{W}^{\text{vir}} = \emptyset, \boldsymbol{T}^{\text{vir}} = \emptyset, \boldsymbol{P}^{\text{vir}} = \emptyset.$

3: **for** $m_i \in \mathcal{M}$ **do**

4:     UAV i sends request for processing task m_i.

5:     USVs and satellites that receive the request will join the set $\boldsymbol{R}^{\text{vir}}$.

6: **end for**

7: **for** $m_i \in \mathcal{M}$ **do**

8:     calculate the values $t_i^{\min}$ and $t_i^{\max}$ using (41).

9:     calculate the values $t_{i,j}^{\text{UAV-min}}$ and $t_{i,j}^{\text{UAV-max}}$ using (42).

10:     calculate the values $\hat{t}_{i,k}^{\text{UAV-min}}$ and $\hat{t}_{i,k}^{\text{UAV-max}}$ using (43).

11:     **if** $t_i^{\min} \leq t_i^{\max}$ & $t_{i,j}^{\text{UAV-min}} \leq t_{i,j}^{\text{UAV-max}}$ & $\hat{t}_{i,k}^{\text{UAV-min}} \leq \hat{t}_{i,k}^{\text{UAV-max}}$ **then**

12:         solve Problem (MCTE-Sub-S) to obtain $t_i^{\text{Ph-I},*}$, $t_{i,j}^{\text{Ph-II},*}, \hat{t}_{i,k}^{\text{Ph-II},*}, p_i^{\text{H},*}, \tau_i^{\text{H},*}$ and assign to $t_i^{\text{Ph-I,vir},*}$, $t_{i,j}^{\text{Ph-II,vir},*}, \hat{t}_{i,k}^{\text{Ph-II,vir},*}, p_i^{\text{H,vir},*}, \tau_i^{\text{H,vir},*}$.

13:         calculate the current matching weight as $w_{m_i, \ell_{m_i}}^{\text{vir}} \leftarrow f_1(t_i^{\text{Ph-I}}) + f_2(t_{i,j}^{\text{Ph-II}}) + f_3(\hat{t}_{i,k}^{\text{Ph-II}}) + f_4(t_i^{\text{Ph-I}}, t_{i,j}^{\text{Ph-II}}, \hat{t}_{i,k}^{\text{Ph-II}}).$

14:     **else**

15:         $\boldsymbol{R}^{\text{vir}} \leftarrow \boldsymbol{R}^{\text{vir}} \setminus \{r_j^{\text{vir}}, r_k^{\text{vir}}\}.$

16:     **end if**

17:     **if** $w_{m_i, \ell_{m_i}}^{\text{vir}} = \infty$ **then**

18:         return infeasible.

19:     **end if**

20: **end for**

21: **if** $\boldsymbol{R}^{\text{vir}} = \emptyset$ **then**

22:     return infeasible.

23: **end if**

24: **Output:** virtual matching weights $\boldsymbol{W}^{\text{vir}}$, virtual time scheduling $\boldsymbol{T}^{\text{vir}}$, virtual transmission power $\boldsymbol{P}^{\text{vir}}$.

---

optimal time scheduling and transmission power, respectively. The offloading decision matrix is defined as $\boldsymbol{X}^{\text{vir}} = \{x_j^{\text{vir}}(m_i), \hat{x}_k^{\text{vir}}(m_i)\}, \forall m_i \in \mathcal{M}, \forall j \in \mathcal{J}, \forall k \in \mathcal{K}$.

Based on the yielded virtual resource allocation in Algorithm 1, we propose Algorithm 2 to obtain the optimal offloading strategy through searching the optimal matching based on the obtained weights.

D. Convergence and Complexity Analysis of Proposed Algorithm

As mentioned in Section IV-A, a vertical architecture is presented to solve Problem (MCTE). In specific, under the given values of $\boldsymbol{x} = \{x_j(m_i)\}_{\forall j \in \mathcal{J}, \forall m_i \in \mathcal{M}}$ and $\hat{\boldsymbol{x}} = \{\hat{x}_k(m_i)\}_{\forall k \in \mathcal{K}, \forall m_i \in \mathcal{M}}$, Problem (MCTE-Sub-S) aims to optimize the time scheduling $\boldsymbol{T}$ and the transmitting power $\boldsymbol{P}$. We prove that Problem (MCTE-Sub-S) is a convex optimization

---

Algorithm 2: Proposed Algorithm for Obtaining Optimal Offloading Strategy.

1: **Input:** $\mathcal{I}, \mathcal{J}, \mathcal{K}, \mathcal{M}, \Gamma, S_{m_i}^{\text{tot}}, \rho_j^{\text{USV}}, \rho_k^{\text{LEO}}, \mu_j^{\text{USV}}, \mu_k^{\text{LEO}},$
   $\mu_i^{\max}, p_i^{\text{UAV-max}}, p_j^{\text{USV-max}}, p_k^{\text{LEO-max}}, W_j^{\text{up}}, \hat{W}_k^{\text{up}}, W_j^{\text{do}},$
   $\hat{W}_k^{\text{do}}, g_{i,j}^{\text{UAV}}, g_{j,i}^{\text{USV}}, \hat{g}_{i,k}^{\text{UAV}}, g_{k,i}^{\text{LEO}}, \forall i, j, k.$
2: **Initialization:** initialize $\boldsymbol{R}^{\text{vir}} = \emptyset, \boldsymbol{W}^{\text{vir}} = \emptyset, \boldsymbol{T}^{\text{vir}} = \emptyset,$
   $\boldsymbol{P}^{\text{vir}} = \emptyset, \boldsymbol{X}^{\text{vir}} = \emptyset.$
3: Invoke Algorithm 1.
4: **while** $\text{rank}(\boldsymbol{X}^{\text{vir}}) \neq |\mathcal{M}|$ **do**
5:    find the smallest $n_i \in \mathcal{M}$ such that $w_{n_i, \ell_{n_i}}^{\text{vir}} = 0.$
6:    set $w_{n_i, \ell_{n_i}}^{\text{vir}} = \min_{\forall \ell_{m_i} \in \boldsymbol{X}} \{w_{n_i, \ell_{m_i}}^{\text{vir}}\}.$
7:    **for** $n_i \in \mathcal{M} \backslash \{m_i\}$ **do**
8:       **if** $\boldsymbol{X}|_{x_{m_i}^{\text{U}}, x_{m_i}^{\text{S}}} = 1$ **then**
9:          **if** $w_{m_i, \ell_{m_i}}^{\text{vir}} < w_{n_i, \ell_{m_i}}^{\text{vir}}$ **then**
10:             set $\boldsymbol{X}|_{x_j(m_i), \hat{x}_k(m_i)} = 1.$
11:             set $\boldsymbol{X}|_{x_j(n_i), \hat{x}_k(n_i)} = 0.$
12:          **else**
13:             set $\boldsymbol{X}|_{x_j(n_i), \hat{x}_k(n_i)} = 1.$
14:             $\mathcal{M} \leftarrow \mathcal{M} \backslash \{n_i\}.$
15:          **end if**
16:       **end if**
17:    **end for**
18:    record the values of $t_i^{\text{Ph-I,vir,}*}, t_{i,j}^{\text{Ph-II,vir,}*},$
       $\hat{t}_{i,k}^{\text{Ph-II,vir,}*}, p_i^{\text{H,vir,}*}, \tau_i^{\text{H,vir,}*}.$
19: **end while**
20: **Output:** virtual offloading decision $\boldsymbol{X}^{\text{vir,}*}$, virtual time
    scheduling $\boldsymbol{T}^{\text{vir,}*}$, virtual transmission power $\boldsymbol{P}^{\text{vir,}*}$.

---

problem, which outputs the optimal solutions. Regarding the Top-problem, based on the obtained values of $\boldsymbol{T}$ and $\boldsymbol{P}$, Problem (MCTE-Top-E) can further optimize the offloading decision $\boldsymbol{X}$ via the bipartite matching approach, which finally derives the optimal solutions.

We explain Algorithm 1 as follows. UAV i first sends request for processing task m_i. The participant which receives the request will join the set $\boldsymbol{R}^{\text{vir}}$ (Lines 3-6). The next process is to determine the feasible matching (Lines 7 to 26). If the time scheduling constraints of (41), (42), (43) are satisfied, we calculate the current weight (Line 19) and store the feasible solution (Line 18). Otherwise, we exclude the infeasible participants which result in infeasible solution (Lines 23-29). After excluding these infeasible participants, we can derive the set of virtual matching weights. The computational complexity of Algorithm 1 is discussed as follows: the number of iterations for computing the weights of all edges is $|\mathcal{M}| \times |\boldsymbol{R}^{\text{vir}}|$. Therefore, the complexity of the proposed Algorithm 1 is $\mathcal{O}(|\mathcal{M}| \times |\boldsymbol{R}^{\text{vir}}|)$.

Algorithm 2 is explained as follows. The stable matching for offloading decision is completed when all tasks have been allocated with virtual resources (Lines 4-19). A task that has not been allocated with a virtual resource will send a request to its preferred virtual resource (the resource with the minimum weight) (Lines 5-6). If the virtual resource is not allocated to other tasks, the virtual resource will accept the request.
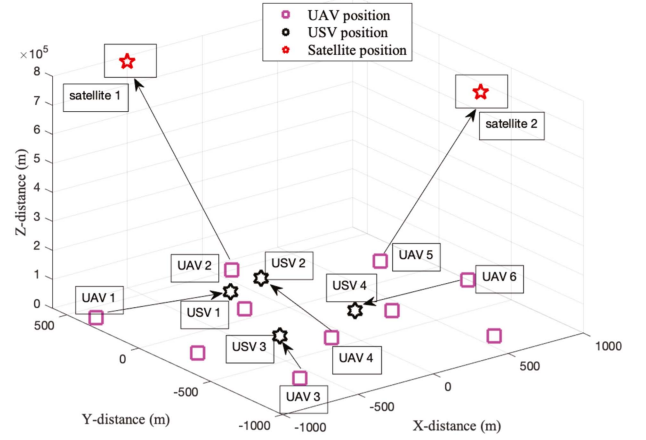

Fig. 5.   Simulation scenario of three-dimensional coordinate in satellite-maritime networks.

Otherwise, the weights of two edges will be compared by the virtual resource (Line 9). Here, $w_{m_i, \ell_{m_i}}^{\text{vir}}$ means the weight of the edge from resource $\ell_{m_i} = (x_j(m_i), \hat{x}_k(m_i)) \in \boldsymbol{X}$ to its currently allocated task m_i, while $w_{n_i, \ell_{m_i}}^{\text{vir}}$ indicates the weight of edge from resource $\ell_{m_i} = (x_j(m_i), \hat{x}_k(m_i)) \in \boldsymbol{X}$ to task n_i which is requesting to match resource ℓ_{m_i}. The virtual resource will determine to match the task with the smallest weight (Lines 10-14). Finally, each task will be allocated with a virtual resource and the stable matching for offloading decision can be achieved by repeating the while-loop until convergence. Algorithm 2 outputs the optimal virtual offloading decision $\boldsymbol{X}^{\text{vir,}*}$, virtual time scheduling $\boldsymbol{T}^{\text{vir,}*}$ and virtual transmission power $\boldsymbol{P}^{\text{vir,}*}$. The computational complexity of Algorithm 2 is discussed as follows. It can be identified that the number of iterations for stable matching (Lines 4-19) is $|\mathcal{M}|^2$. Therefore, the complexity of the proposed Algorithm 2 is $\mathcal{O}(|\mathcal{M}|^2)$.
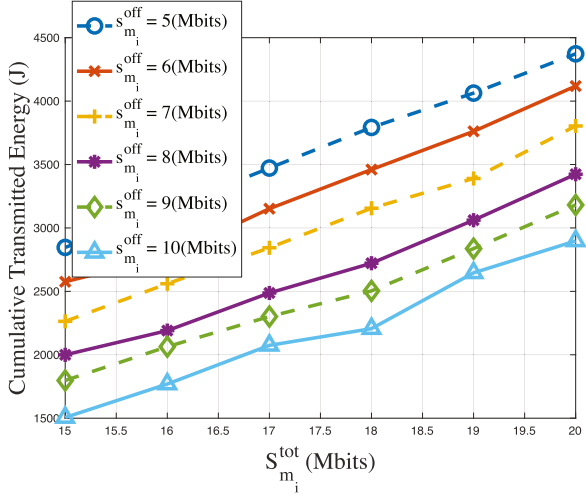
V. PERFORMANCE EVALUATION

In this section, we conduct simulation experiments to validate the effectiveness of the proposed algorithms. The simulation setup is first introduced, followed by the numerical results and analysis.

A. Simulation Setup

In the simulations, we consider a three-dimensional initial coordinate scenario in satellite-maritime networks, as shown in Fig. 5. Ten UAVs are hovering in the air to perceive ocean information. The positions of UAVs are set as $(100, 500)$m, $(-900, 400)$m, $(-200, 100)$m, $(800, 200)$m, $(-100, -400)$m, $(400, -300)$m, $(-600, -700)$m, $(600, -800)$m, $(-800, -200)$m, and $(1000, -200)$ m, respectively. The hovering height of UAVs is set to 200m. Four USVs are deployed on the sea surface. The positions of USVs are set as $(150, 350)$m, $(-100, 300)$m, $(250, -200)$m, $(-300, -250)$ m, respectively. Two LEO satellites are available in the space for communicating with UAVs. UAVs and USVs maintain the same position unchanged during the task offloading process. According to [48], [49], other system parameter settings are provided
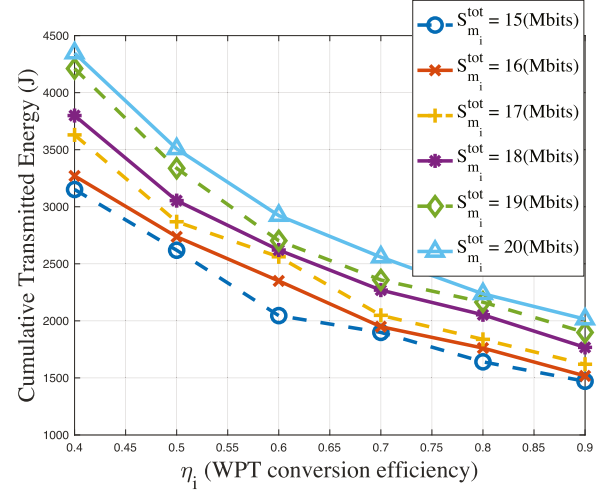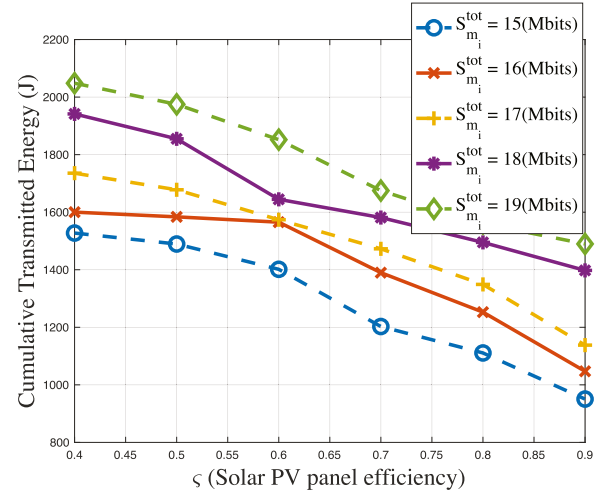
TABLE III
SYSTEM PARAMETER SETTINGS

Parameters	Values	Parameters	Values
I	10	H_i	200m
J	4	$R_{i,k}$	784km
K	2	R_e	6371km
κ_i	10^{-18}	$\alpha_{i,k}$	25°
ρ_i^{UAV}	$[1,5] \times 10^3$cycles/s	v_k	27400km/h
μ_i^{UAV}	$[1,10] \times 10^3$cycles	δ_0	-50dB
ρ_j^{USV}	$[1,5] \times 10^6$cycles/s	$d^{\min}$	50m
μ_j^{USV}	$[1,5] \times 10^7$cycles	$\sigma_i^2, \sigma_j^2, \sigma_k^2$	10^{-9}dBm
ρ_k^{LEO}	$[1,4] \times 10^9$cycles/s	p^{coe}	0.02
μ_k^{LEO}	$[1,4] \times 10^{10}$cycles	A^{den}	1.5kg/m^3
$S_{m_i}^{\mathrm{tot}}$	$[11,20]$Mbits	i^{rat}	0.05
$s_{m_i}^{\mathrm{off}}$	$[1,10]$Mbits	Ω	0.51m^2
ϵ_i	0.1	B	50m/s
η_i	0.8	C	0.5m
W_j^{up}	20MHz	F	0.1
W_j^{do}	100MHz	w	$[11,20]$Newton
$\hat{W}_k^{\mathrm{up}}$	10MHz	ς	0.8
$\hat{W}_k^{\mathrm{do}}$	50MHz	Υ_s	0.426×0.214m^2
λ	0.083nm [50]	N_s	2
θ_{rain}	6dB [50]	I_{pv}	150W/m^2

Fig. 7. The changes of cumulative transmitted energy with WPT conversion efficiency η_i.

Fig. 8. The changes of cumulative transmitted energy with the efficiency of solar PV panel ς.

Fig. 6. The changes of cumulative transmitted energy with the total workloads $S_{m_i}^{\mathrm{tot}}$ of UAV i.

in Table III. The results are obtained with a PC of Intel(R) Core(TM) i7-9700 CPU@3.00 GHz.

B. Numerical Results and Analysis

In the numerical results, we first evaluate the offloading strategy of our proposed algorithms. Fig. 6 shows the changes of cumulative transmitted energy (i.e., objective function in Problem (MCTE)) with the total workloads $S_{m_i}^{\mathrm{tot}}$ of UAV i. It can be seen from Fig. 6 that the cumulative transmitted energy is increasing with the total workloads of UAV i. Moreover, the greater the offloading workloads (i.e., $s_{m_i}^{\mathrm{off}}$), the lower the cumulative transmitted energy. The reasons are as follows. When increasing the total workloads of UAV i, more energy will be

consumed for offloading and processing the workloads of UAV i, which leads to high energy consumption, i.e., more cumulative transmitted energy to UAV i.

Fig. 7 illustrates the changes of cumulative transmitted energy with WPT conversion efficiency η_i. We can see that the higher WPT conversion efficiency η_i makes the lower cumulative transmitted energy to UAV i. This is because a higher WPT conversion efficiency η_i results in a greater energy harvested by UAV i, thereby reducing the cumulative energy transmitted to it. Moreover, the higher total workloads of UAV i leads to the greater cumulative transmitted energy. The reasons are similar to the description in Fig. 6.

Fig. 8 depicts the changes of cumulative transmitted energy with the efficiency of solar PV panel ς. It can be derived from Fig. 8 that the larger efficiency of solar PV panel ς leads to the lower cumulative transmitted energy. The reasons can be explained as follows. A high solar PV panel efficiency ς can increase the energy harvested by UAV i from solar energy, thereby reducing the cumulative transmitted energy. In addition, similar
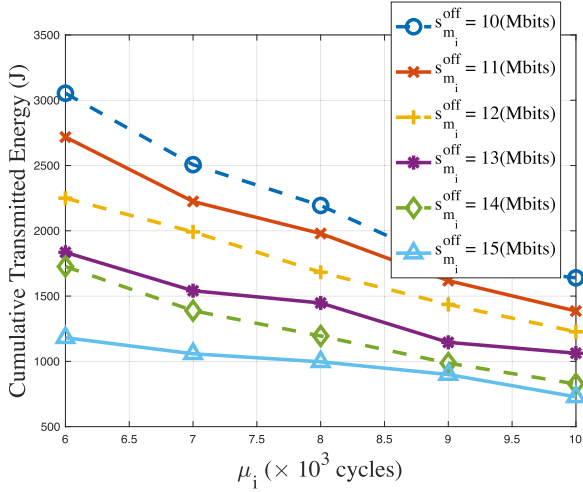
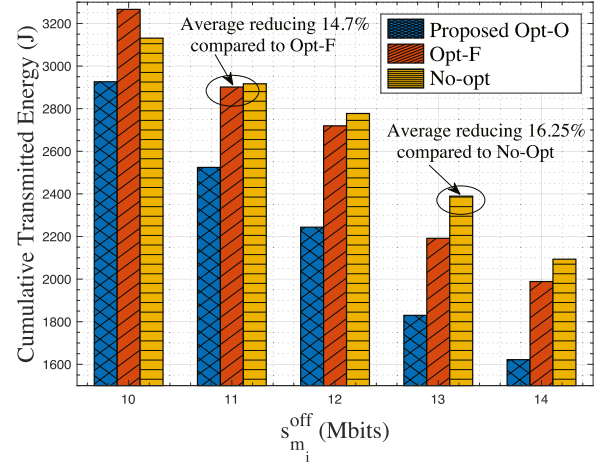Fig. 9. The changes of cumulative transmitted energy with the number of CPU cycles μ_i of UAV i.

Fig. 10. Performance comparison of cumulative transmitted energy for the proposed algorithm, Opt-F, and No-opt under different offloading workloads $s_{m_i}^{\text{off}}$.

Fig. 11. Performance comparison of cumulative transmitted energy for the proposed algorithm, Opt-F, and No-opt under different number of CPU cycles μ_i.

to the reasons described in Fig. 6, the increasing workloads of UAV i causes the raising of cumulative transmitted energy.

Fig. 9 shows the changes of cumulative transmitted energy with the number of CPU cycles μ_i of UAV i. From Fig. 9, we can see that as the number of CPU cycles μ_i of UAV i increases, the cumulative transmitted energy is decreased. It can be explained that by increasing the number of CPU cycles μ_i of UAV i, the local computing energy in Phase I will be decreased according to (13), resulting in low cumulative transmitted energy. Furthermore, the cumulative transmitted energy is reduced when increasing the offloading workloads $s_{m_i}^{\text{off}}$, the reason is similar to the explanation in Fig. 6.

In the following, we conduct performance evaluation of our proposed algorithm by comparing it with different matching schemes, which are listed as follows. *Optimized Fixed Matching (Opt-F):* In this scheme, UAVs select the determined USVs or satellites based on the predefined number for offloading their workloads. The offloading strategy is according to the proposed algorithm. *No Optimized Matching (No-Opt):* In this scheme, UAVs randomly choose USVs or satellites to offload their workloads.

Fig. 10 demonstrates the performance comparison of cumulative transmitted energy for the proposed algorithm, Opt-F, and No-opt un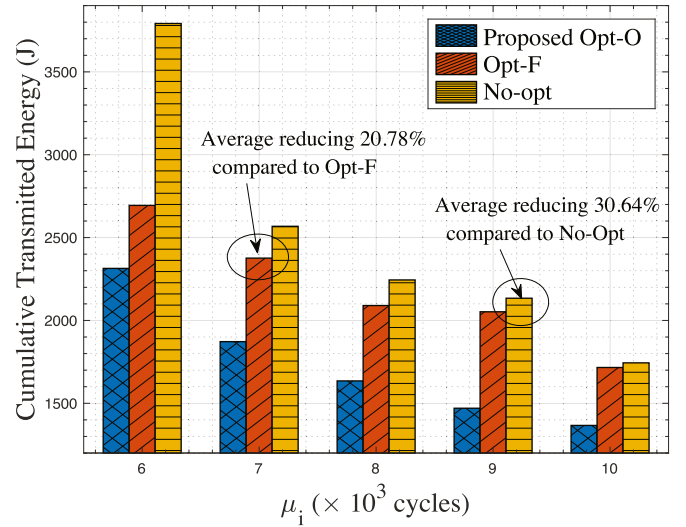der different offloading workloads $s_{m_i}^{\text{off}}$. It can be seen from Fig. 10 that the proposed algorithm can attain the lowest cumulative transmitted energy among three schemes, and the cumulative transmitted energy is decreasing with the offloading workloads $s_{m_i}^{\text{off}}$. The reason is that the proposed algorithm takes the optimal offloading strategy into account, thereby reducing the cumulative transmitted energy for UAVs. The Opt-F may not determine the optimal strategy to offload UAVs' workloads. The No-Opt randomly determines the offloading strategy, which results in the random strategy and high cumulative transmitted energy.

Fig. 11 illustrates the performance comparison of cumulative transmitted energy for the proposed algorithm, Opt-F, and No-opt under different number of CPU cycles μ_i. We can attain

that the proposed algorithm has the best performance compared to other schemes due to the fact that our proposed algorithm jointly optimizes the offloading strategy, the time scheduling and the transmission power. Moreover, the cumulative transmitted energy is decreasing with the number of cycles μ_i, the reason is similar to the description of Fig. 9.

Fig. 12 depicts the performance comparison of cumulative transmitted energy for the proposed algorithm, Opt-F, and No-opt by exploiting the changes of WPT conversion efficiency η_i. From Fig. 12, it can be obtained that our proposed algorithm outperforms Opt-F, and No-opt because the proposed algorithm optimizes the offloading strategy, thus reducing the cumulative transmitted energy. In addition, as the WPT conversion efficiency η_i raises, the cumulative transmitted energy is decreasing. The reasons are similar to the explanation in Fig. 7.

Fig. 13 shows the performance comparison of cumulative transmitted energy for the proposed algorithm, Opt-F, and

TABLE IV
COMPARISON OF THE PROPOSED OFFLOADING SCHEME AND BASELINE SCHEMES

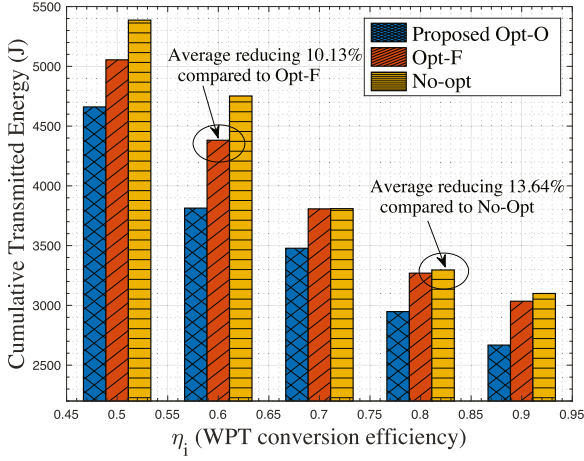| Comparison schemes	$x_j(m_i)$	$\hat{x}_k(m_i)$	Computing type
Myopic [51]	$0, \forall j \in \mathcal{J}, m_i \in \mathcal{M}$	$0, \forall k \in \mathcal{K}, m_i \in \mathcal{M}$	Always computing on UAV
"Always on" [46]	$0, \forall j \in \mathcal{J}, m_i \in \mathcal{M}$	$1, \forall k \in \mathcal{K}, m_i \in \mathcal{M}$	Always computing on Satellite
	$1, \forall j \in \mathcal{J}, m_i \in \mathcal{M}$	$0, \forall k \in \mathcal{K}, m_i \in \mathcal{M}$	Always computing on USV
"Always average"	$0, \forall j \in \mathcal{J}, m_i \in \mathcal{M}$	$1, \forall k \in \mathcal{K}, m_i \in \mathcal{M}$	Average computing on Satellite and UAV
	$1, \forall j \in \mathcal{J}, m_i \in \mathcal{M}$	$0, \forall k \in \mathcal{K}, m_i \in \mathcal{M}$	Average computing on USV and UAV
Proposed optimal offloading (Opt-O)	$0, \forall j \in \mathcal{J}, m_i \in \mathcal{M}$	$1, \forall k \in \mathcal{K}, m_i \in \mathcal{M}$	Computing on UAV and Satellite
	$1, \forall j \in \mathcal{J}, m_i \in \mathcal{M}$	$0, \forall k \in \mathcal{K}, m_i \in \mathcal{M}$	Computing on UAV and USV

Fig. 12. Performance comparison of cumulative transmitted energy for the proposed algorithm, Opt-F, and No-opt by exploiting the changes of WPT conversion efficiency η_i.
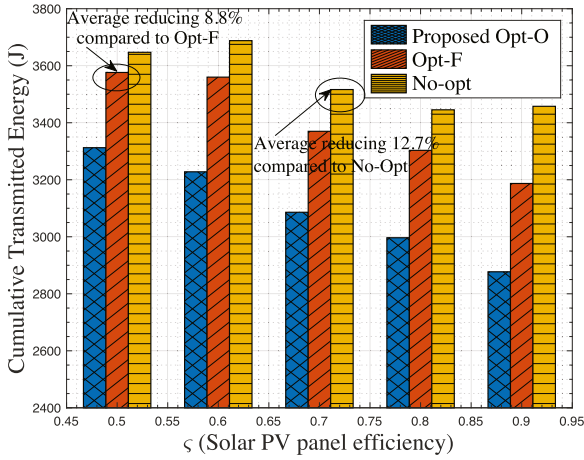

Fig. 13. Performance comparison of cumulative transmitted energy for the proposed algorithm, Opt-F, and No-opt by exploiting the changes of solar PV panel efficiency ς.

Fig. 14. Performance evaluation for the total workloads $S_{m_i}^{\text{tot}}$ under different baseline schemes.

No-opt by exploiting the changes of solar PV panel efficiency ς. We can see that the cumulative transmitted energy in the proposed algorithm is lower than that of Opt-F and No-opt. This is due to the fact that our proposed algorithm considers the optimal offloading strategy to minimize the cumulative transmitted energy. Furthermore, the cumulative transmitted energy is decreasing with the value of ς. This can be explained by Fig. 8.
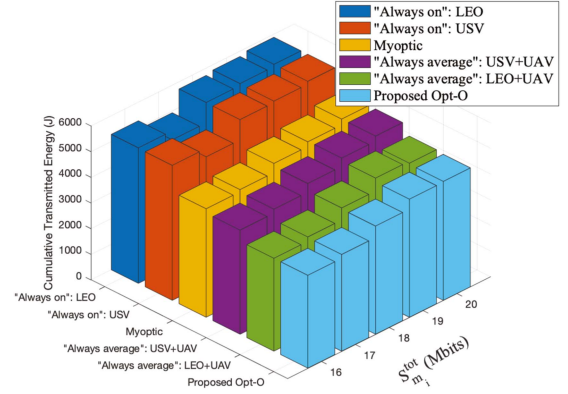
Finally, we provide the performance comparison of our proposed scheme with the following baseline schemes, i.e., Myopic [50], "Always on" [45] means that the total workloads of UAV are fully offloaded to USVs or satellites to process. "Always average" denotes that the total workloads of UAV are uniformly offloaded to USVs or satellites. The comparison of the proposed offloading scheme and baseline schemes is provided in Table IV.

Fig. 14 illustrates the performance evaluation for the total workloads $S_{m_i}^{\text{tot}}$ under different baseline schemes. The result in Fig. 14 demonstrates the effectiveness of our proposed algorithm in comparison with baseline schemes. The reasons are as follows. "Myopic" requires UAVs to complete the tasks locally at each time. This increases the energy consumption of local computing. "Always on" requires UAVs to fully offload tasks to USVs or satellites. The transmission consumption for USV and satellite is high. "Always average" does not consider the offloading strategy. This also raises the energy consumption during offloading. Our proposed algorithm jointly optimizes the offloading strategy and resource allocation, which reduces the cumulative transmitted energy.

Fig. 15 demonstrates the performance evaluation for the number of CPU cycles μ_i under different baseline schemes. It can be seen from Fig. 15 that the performance of our proposed algorithm is superior to baseline schemes. The reasons are similar to Fig. 14.

Fig. 16 shows the performance evaluation for the WPT conversion efficiency η_i under different baseline schemes. We can find that the cumulative transmitted energy for the proposed
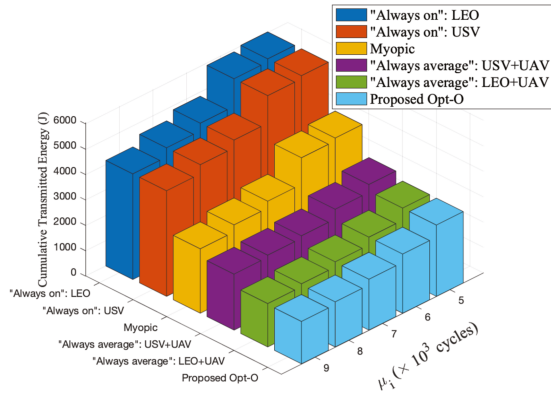
Fig. 15. Performance evaluation for the number of CPU cycles μ_i under different baseline schemes.
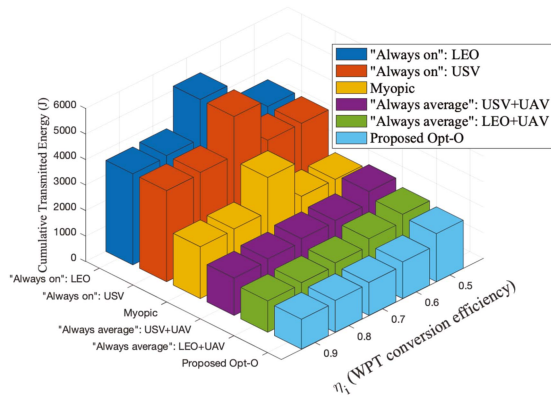

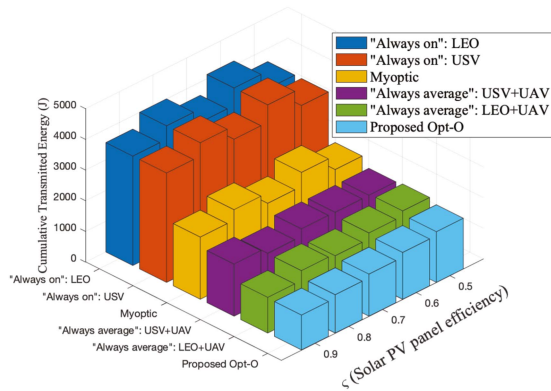Fig. 16. Performance evaluation for the WPT conversion efficiency η_i under different baseline schemes.

Fig. 17. Performance evaluation for the solar PV panel efficiency ς under different baseline schemes.

algorithm is the lowest among baseline schemes due to the fact that the proposed algorithm takes the optimal offloading strategy into account.

Fig. 17 depicts the performance evaluation for the solar PV panel efficiency ς under different baseline schemes. From Fig. 17, it can be derived that our proposed algorithm can minimize the cumulative transmitted energy by optimizing the offloading strategy.

VI. CONCLUSION

In this paper, we have proposed an energy efficient multi-access computing offloading scheme in satellite-maritime networks to improve maritime service efficiency. Specifically, we have presented a heterogeneous satellite-maritime network framework, where LEO satellites and USVs equipped with computing capacities can execute task computing for UAVs. To improve the resource utilization, we have proposed a hybrid harvesting-and-offloading scheme. In the harvesting duration, USVs can charge UAVs via WPT to enhance the offloading endurance. In the offloading duration, UAVs can offload task to LEO satellites and USVs via multi-access mode to improve the offloading efficiency. Then, we have formulated an optimization problem to jointly optimize the offloading decision, the time scheduling, and the transmitting power, with the objective of minimizing the cumulative transmitted energy. To obtain the optimal solutions, we have presented a vertical architecture. Finally, simulation results have demonstrated the effectiveness and efficiency of our proposed algorithm compared to baseline schemes. For the future work, we will further investigate the secure computing offloading scheme in space-air-ground integrated networks to guarantee the quality of maritime services.

REFERENCES

[1] M. Jahanbakht, W. Xiang, L. Hanzo, and M. R. Azghadi, "Internet of underwater things and big marine data analytics—A comprehensive survey," *IEEE Commun. Surveys Tuts.*, vol. 23, no. 2, pp. 904–956, Second Quarter, 2021.

[2] H. Guo, J. Li, J. Liu, N. Tian, and N. Kato, "A survey on space-air-ground-sea integrated network security in 6G," *IEEE Commun. Surveys Tuts.*, vol. 24, no. 1, pp. 53–87, First Quarter, 2022.

[3] J. Xu, M. A. Kishk, and M.-S. Alouini, "Space-air-ground-sea integrated networks: Modeling and coverage analysis," *IEEE Trans. Wireless Commun.*, vol. 22, no. 9, pp. 6298–6313, Sep. 2023.

[4] A. Alsharoa and M.-S. Alouini, "Improvement of the global connectivity using integrated satellite-airborne-terrestrial networks with resource optimization," *IEEE Trans. Wireless Commun.*, vol. 19, no. 8, pp. 5088–5100, Aug. 2020.

[5] X. Qin, T. Ma, Z. Tang, X. Zhang, H. Zhou, and L. Zhao, "Service-aware resource orchestration in ultra-dense leo satellite-terrestrial integrated 6G: A service function chain approach," *IEEE Trans. Wireless Commun.*, vol. 22, no. 9, pp. 6003–6017, Sep. 2023.

[6] J. Liu, P. Tong, X. Wang, B. Bai, and H. Dai, "UAV-aided data collection for information freshness in wireless sensor networks," *IEEE Trans. Wireless Commun.*, vol. 20, no. 4, pp. 2368–2382, Apr. 2021.

[7] Y. Li et al., "Data collection maximization in IoT-sensor networks via an energy-constrained UAV," *IEEE Trans. Mobile Comput.*, vol. 22, no. 1, pp. 159–174, Jan. 2023.

[8] M. Dai, C. Dou, Y. Wu, L. Qian, R. Lu, and T. Q. S. Quek, "Multi-UAV aided multi-access edge computing in marine communication networks: A joint system-welfare and energy-efficient design," *IEEE Trans. Commun.*, vol. 72, no. 9, pp. 5517–5531, Sep. 2024.

[9] X. Zhou, C. K. Ho, and R. Zhang, "Wireless power meets energy harvesting: A joint energy allocation approach in OFDM-based system," *IEEE Trans. Wireless Commun.*, vol. 15, no. 5, pp. 3481–3491, May 2016.

[10] R. Guida, E. Demirors, N. Dave, and T. Melodia, "Underwater ultrasonic wireless power transfer: A battery-less platform for the internet of underwater things," *IEEE Trans. Mobile Comput.*, vol. 21, no. 5, pp. 1861–1873, May 2022.

[11] L. Xie, X. Cao, J. Xu, and R. Zhang, "UAV-enabled wireless power transfer: A tutorial overview," *IEEE Trans. Green Commun. Netw.*, vol. 5, no. 4, pp. 2042–2064, Dec. 2021.

[12] J. Shi, P. Cong, L. Zhao, X. Wang, S. Wan, and M. Guizani, "A two-stage strategy for UAV-enabled wireless power transfer in unknown environments," *IEEE Trans. Mobile Comput.*, vol. 23, no. 2, pp. 1785–1802, Feb. 2024.

[13] R. Malik and M. Vu, "On-request wireless charging and partial computation offloading in multi-access edge computing systems," *IEEE Trans. Wireless Commun.*, vol. 20, no. 10, pp. 6665–6679, Oct. 2021.

[14] P. Wu, F. Xiao, H. Huang, and R. Wang, "Load balance and trajectory design in multi-UAV aided large-scale wireless rechargeable networks," *IEEE Trans. Veh. Technol*, vol. 69, no. 11, pp. 13756–13767, Nov. 2020.

[15] S. K. Singh, K. Agrawal, K. Singh, A. Bansal, C.-P. Li, and Z. Ding, "On the performance of laser-powered UAV-assisted SWIPT enabled multiuser communication network with hybrid NOMA," *IEEE Trans. Commun.*, vol. 70, no. 6, pp. 3912–3929, Jun. 2022.

[16] Y. Hu, X. Yuan, J. Xu, and A. Schmeink, "Optimal 1D trajectory design for UAV-enabled multiuser wireless power transfer," *IEEE Trans. Commun.*, vol. 67, no. 8, pp. 5674–5688, Aug. 2019.

[17] Y. Hu, X. Yuan, G. Zhang, and A. Schmeink, "Sustainable wireless sensor networks with UAV-enabled wireless power transfer," *IEEE Trans. Veh. Technol*, vol. 70, no. 8, pp. 8050–8064, Aug. 2021.

[18] L. Zong, H. Wang, and G. Luo, "Transmission control over satellite network for marine environmental monitoring system," *IEEE Trans. Intell. Transp. Syst.*, vol. 23, no. 10, pp. 19668–19675, Oct. 2022.

[19] Y. Cai, S. Wu, J. Luo, J. Jiao, N. Zhang, and Q. Zhang, "Age-oriented access control in GEO/LEO heterogeneous network for marine IoRT: A deep reinforcement learning approach," *IEEE Internet Things J.*, vol. 9, no. 24, pp. 24919–24932, Dec. 2022.

[20] C. Garibotto, A. Sciarrone, F. Lavagetto, L. Pronzati, A. Baljak, and G. Tagliabue, "Performance analysis of an IoT-based personal vocal assistant for cruise ships over satellite networks," *IEEE Internet Things J.*, vol. 9, no. 16, pp. 14857–14866, Aug. 2022.

[21] X. Hu et al., "Performance analysis of end-to-end LEO satellite-aided shore-to-ship communications: A stochastic geometry approach," *IEEE Trans. Wireless Commun.*, vol. 23, no. 9, pp. 11753–11769, Sep. 2024.

[22] X. Li, W. Feng, Y. Chen, C.-X. Wang, and N. Ge, "Maritime coverage enhancement using UAVs coordinated with hybrid satellite-terrestrial networks," *IEEE Trans. Commun.*, vol. 68, no. 4, pp. 2355–2369, Apr. 2020.

[23] H. Zeng et al., "Collaborative computation offloading for UAVs and USV fleets in communication networks," in *Proc. Int. Wireless Commun. Mobile Comput.*, 2022, pp. 949–954.

[24] C. Zeng et al., "Collaborative USV-buoy enabled maritime wireless networks: Cache-aided beamforming and trajectory design," *IEEE Trans. Commun.*, early access, Mar. 14, 2025, doi: 10.1109/TCOMM.2025.3551632.

[25] M. Cheng, Q. Guan, Q. Wang, F. Ji, and T. Q. S. Quek, "FER-restricted AUV-relaying data collection in underwater acoustic sensor networks," *IEEE Trans. Wireless Commun.*, vol. 22, no. 12, pp. 9131–9142, Dec. 2023.

[26] C. Zeng, J.-B. Wang, C. Ding, H. Zhang, M. Lin, and J. Cheng, "Joint optimization of trajectory and communication resource allocation for unmanned surface vehicle enabled maritime wireless networks," *IEEE Trans. Commun.*, vol. 69, no. 12, pp. 8100–8115, Dec. 2021.

[27] M. Dai, Y. Wu, L. Qian, Z. Su, B. Lin, and N. Chen, "UAV-assisted multi-access computation offloading via hybrid NOMA and FDMA in marine networks," *IEEE Trans. Netw. Sci. Eng.*, vol. 10, no. 1, pp. 113–127, Jan./Feb. 2023.

[28] C. Zeng, J.-B. Wang, C. Ding, M. Lin, and J. Wang, "MIMO unmanned surface vessels enabled maritime wireless network coexisting with satellite network: Beamforming and trajectory design," *IEEE Trans. Commun.*, vol. 71, no. 1, pp. 83–100, Jan. 2023.

[29] X. Fang et al., "NOMA-based hybrid satellite-UAV-terrestrial networks for 6G maritime coverage," *IEEE Trans. Wireless Commun.*, vol. 22, no. 1, pp. 138–152, Jan. 2023.

[30] Q. Xu, Z. Su, R. Lu, and S. Yu, "Ubiquitous transmission service: Hierarchical wireless data rate provisioning in space-air-ocean integrated networks," *IEEE Trans. Wireless Commun.*, vol. 21, no. 9, pp. 7821–7836, Sep. 2022.

[31] C. Lin, G. Han, J. Jiang, C. Li, S. B. H. Shah, and Q. Liu, "Underwater pollution tracking based on software-defined multi-tier edge computing in 6G-based underwater wireless networks," *IEEE J. Sel. Areas Commun.*, vol. 41, no. 2, pp. 491–503, Feb. 2023.

[32] Y. Ma, W. Liang, and W. Xu, "Charging utility maximization in wireless rechargeable sensor networks by charging multiple sensors simultaneously," *IEEE/ACM Trans. Netw.*, vol. 26, no. 4, pp. 1591–1604, Aug. 2018.

[33] L. Sun, L. Wan, K. Liu, and X. Wang, "Cooperative-evolution-based WPT resource allocation for large-scale cognitive industrial IoT," *IEEE Trans. Ind. Informat.*, vol. 16, no. 8, pp. 5401–5411, Aug. 2020.

[34] K. A. Mahmoodi and M. Uysal, "Energy aware trajectory optimization of solar powered AUVs for optical underwater sensor networks," *IEEE Trans. Commun.*, vol. 70, no. 12, pp. 8258–8269, Dec. 2022.

[35] X. Yuan, H. Jiang, Y. Hu, and A. Schmeink, "Joint analog beamforming and trajectory planning for energy-efficient UAV-enabled nonlinear wireless power transfer," *IEEE J. Sel. Areas Commun.*, vol. 40, no. 10, pp. 2914–2929, Oct. 2022.

[36] Y. K. Tun, T. N. Dang, K. Kim, M. Alsenwi, W. Saad, and C. S. Hong, "Collaboration in the sky: A distributed framework for task offloading and resource allocation in multi-access edge computing," *IEEE Internet Things J.*, vol. 9, no. 23, pp. 24221–24235, Dec. 2022.

[37] P. A. Apostolopoulos, G. Fragkos, E. E. Tsiropoulou, and S. Papavassiliou, "Data offloading in UAV-assisted multi-access edge computing systems under resource uncertainty," *IEEE Trans. Mobile Comput.*, vol. 22, no. 1, pp. 175–190, Jan. 2023.

[38] X. Diao, W. Yang, L. Yang, and Y. Cai, "UAV-relaying-assisted multi-access edge computing with multi-antenna base station: Offloading and scheduling optimization," *IEEE Trans. Veh. Technol*, vol. 70, no. 9, pp. 9495–9509, Sep. 2021.

[39] H. Peng and X. Shen, "Multi-agent reinforcement learning based resource management in MEC- and UAV-assisted vehicular networks," *IEEE J. Sel. Areas Commun.*, vol. 39, no. 1, pp. 131–141, Jan. 2021.

[40] C. Kim, H.-H. Choi, and K. Lee, "Joint optimization of trajectory and resource allocation for multi-UAV-enabled wireless-powered communication networks," *IEEE Trans. Commun.*, vol. 72, no. 9, pp. 5752–5764, Sep. 2024.

[41] H. Pan, Y. Liu, G. Sun, J. Fan, S. Liang, and C. Yuen, "Joint power and 3D trajectory optimization for UAV-enabled wireless powered communication networks with obstacles," *IEEE Trans. Commun.*, vol. 71, no. 4, pp. 2364–2380, Apr. 2023.

[42] Z. Ning, H. Ji, X. Wang, E. C. H. Ngai, L. Guo, and J. Liu, "Joint optimization of data acquisition and trajectory planning for UAV-assisted wireless powered Internet of Things," *IEEE Trans. Mobile Comput.*, vol. 24, no. 2, pp. 1016–1030, Feb. 2025.

[43] Z. Y. Zhao, Y. L. Che, S. Luo, G. Luo, K. Wu, and V. C. M. Leung, "On designing multi-UAV aided wireless powered dynamic communication via hierarchical deep reinforcement learning," *IEEE Trans. Mobile Comput.*, vol. 23, no. 12, pp. 13991–14004, Dec. 2024.

[44] C. Huang, G. Chen, P. Xiao, Y. Xiao, Z. Han, and J. A. Chambers, "Joint offloading and resource allocation for hybrid cloud and edge computing in SAGINs: A decision assisted hybrid action space deep reinforcement learning approach," *IEEE J. Sel. Areas Commun.*, vol. 42, no. 5, pp. 1029–1043, May 2024.

[45] S. Jung, S. Jeong, J. Kang, and J. Kang, "Marine IoT systems with space–air–sea integrated networks: Hybrid LEO and UAV edge computing," *IEEE Internet Things J.*, vol. 10, no. 23, pp. 20498–20510, Dec. 2023.

[46] Z. Wang, J. Du, C. Jiang, Y. Ren, and X.-P. Zhang, "UAV-assisted target tracking and computation offloading in USV-based MEC networks," *IEEE Trans. Mobile Comput.*, vol. 23, no. 12, pp. 11389–11405, Dec. 2024.

[47] T. Ma et al., "UAV-LEO integrated backbone: A ubiquitous data collection approach for B5G internet of remote things networks," *IEEE J. Sel. Areas Commun.*, vol. 39, no. 11, pp. 3491–3505, Nov. 2021.

[48] Q. Tang, Z. Fei, B. Li, and Z. Han, "Computation offloading in LEO satellite networks with hybrid cloud and edge computing," *IEEE Internet Things J.*, vol. 8, no. 11, pp. 9164–9176, Jun. 2021.

[49] S. Gu, X. Sun, Z. Yang, T. Huang, W. Xiang, and K. Yu, "Energy-aware coded caching strategy design with resource optimization for satellite-UAV-vehicle-integrated networks," *IEEE Internet Things J.*, vol. 9, no. 8, pp. 5799–5811, Apr. 2022.

[50] F. Wang, J. Xu, and S. Cui, "Optimal energy allocation and task offloading policy for wireless powered mobile edge computing systems," *IEEE Trans. Wireless Commun.*, vol. 19, no. 4, pp. 2443–2459, Apr. 2020.

[51] Y. Zeng, J. Xu, and R. Zhang, "Energy minimization for wireless communication with rotary-wing UAV," *IEEE Trans. Wireless Commun.*, vol. 18, no. 4, pp. 2329–2345, Apr. 2019.

[52] K. Zheng, F. Liu, Q. Zheng, W. Xiang, and W. Wang, "A graph-based cooperative scheduling scheme for vehicular networks," *IEEE Trans. Veh. Technol*, vol. 62, no. 4, pp. 1450–1458, May 2013.

[53] L. Liang, S. Xie, G. Y. Li, Z. Ding, and X. Yu, "Graph-based resource sharing in vehicular communication," *IEEE Trans. Wireless Commun.*, vol. 17, no. 7, pp. 4579–4592, Jul. 2018.
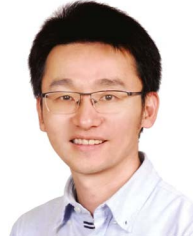
Minghui Dai (Member, IEEE) received the PhD degree from Shanghai University, Shanghai, China, in 2021. He is currently an assistant professor with the School of Computer Science and Technology, Donghua University, Shanghai, China. From 2021 to 2024, he was a post-doctoral fellow with the State Key Laboratory of Internet of Things for Smart City, University of Macau, Macau. His research interests include the general area of wireless network architecture and vehicular networks.

Yixuan Wang received the BSc degree in software engineering from the Jiangsu University, Zhenjiang, China, in 2023. He is currently working toward the MS degree with the Department of Computer Science and Technology, University of Donghua, Shanghai, China. His research interests include resource management for wireless networks, multi access edge computing, and the mobile social networks.

Shan Chang (Member, IEEE) received the PhD degree in computer software and theory from Xi'an Jiaotong University, Xi'an, China, in 2012. From 2009 to 2010, she was a visiting scholar with the Department of Computer Science and Engineering, Hong Kong University of Science and Technology, Hong Kong. She was also a visiting scholar with BBCR Research Lab, University of Waterloo, Waterloo, ON, Canada, from 2010 to 2011. She is currently a professor with the Department of Computer Science and Technology, Donghua University, Shanghai, China. Her research interests include security and privacy in mobile networks and sensor networks. She is a member of IEEE Computer Society, Communication Society, and Vehicular Technology Society.

Zhou Su (Senior Member, IEEE) received the PhD degree from Waseda University, Tokyo, Japan, in 2003. He has published technical papers, including top journals and top conferences, such as the *IEEE Journal on Selected Areas in Communications*, *IEEE Transactions on Information Forensics and Security*, *IEEE Transactions on Dependable and Secure Computing*, *IEEE Transactions on Mobile Computing*, *IEEE/ACM Transactions on Networking*, and Infocom. His research interests include multimedia communication, wireless communication, and network traffic. He received the Best Paper Award of International Conference IEEE ICC2020, IEEE BigdataSE2019, and IEEE CyberSciTech 2017. He is an associate editor of the *IEEE Internet of Things Journal*, *IEEE Open Journal of Computer Society*, and *IET Communications*.